

A Bispidol Chelator with a Phosphonate Pendant Arm: Synthesis, Cu(II) Complexation, and (64)Cu Labeling

Raphaël Gillet, Amandine Roux, Jérémy Brandel, Sandrine Huclier-Markai, Franck Camerel, Olivier Jeannin, Aline M. Nonat, Loïc J. Charbonnière

▶ **To cite this version:**

Raphaël Gillet, Amandine Roux, Jérémy Brandel, Sandrine Huclier-Markai, Franck Camerel, et al.. A Bispidol Chelator with a Phosphonate Pendant Arm: Synthesis, Cu(II) Complexation, and (64)Cu Labeling. Inorganic Chemistry, 2017, 56 (19), pp.11738-11752. 10.1021/acs.inorgchem.7b01731 . hal-01617953

HAL Id: hal-01617953

https://univ-rennes.hal.science/hal-01617953

Submitted on 1 Dec 2017

HAL is a multi-disciplinary open access archive for the deposit and dissemination of scientific research documents, whether they are published or not. The documents may come from teaching and research institutions in France or abroad, or from public or private research centers.

L'archive ouverte pluridisciplinaire **HAL**, est destinée au dépôt et à la diffusion de documents scientifiques de niveau recherche, publiés ou non, émanant des établissements d'enseignement et de recherche français ou étrangers, des laboratoires publics ou privés.

Bispidol chelator with phosphonate pendant arm: synthesis, Cu(II) complexation and ^{64}Cu labeling

Raphaël Gillet,† Amandine Roux,† Jérémy Brandel,‡ Sandrine Huclier-Markai,§ ǂ Franck Camerel,ð Olivier Jeannin, ð Aline M. Nonat,†, Loïc J. Charbonnière*†*

†Laboratoire d'Ingénierie Moléculaire Appliquée à l'Analyse, Université de Strasbourg, CNRS, IPHC UMR 7178, F-67000 Strasbourg, France.

‡ Laboratoire de Reconnaissance et Procédés de Séparation Moléculaire, Université de Strasbourg, CNRS, IPHC UMR 7178, F-67000 Strasbourg, France.

§ GIP Arronax, 1 rue Aronnax, CS 10112, F-44817 Saint-Herblain, France.

ǂ Subatech Laboratory, UMR 6457, Ecole des Mines de Nantes, IN2P3/CNRS, Université de Nantes, 4 rue Alfred Kastler, F-44307 Nantes, France.

ð Laboratoire Matière Condensée et Systèmes Électroactifs, Institut des Sciences Chimiques de Rennes, UMR-CNRS 6226, 263 Avenue du Général Leclerc, CS 74205, F-35042 Rennes Cedex, France

aline.nonat@unistra.fr, l.charbonn@unistra.fr

KEYWORDS : ^{64}Cu / selectivity / kinetic inertness / bispidine / phosphonate/ radiolabelling / PET

ABSTRACT. Here we present the synthesis and characterization of a new bispidine (3,7-diazabicyclo[3.3.1]nonane) ligand with N-methanephosphonate substituents (**L_2**). Its physico-chemical properties in water, as well as those of the corresponding Cu(II) and Zn(II) complexes,

have been evaluated by using UV-visible absorption spectroscopy, potentiometry, ^{1}H and ^{31}P NMR and cyclic voltammetry. Radiolabelling experiments with $^{64}Cu(II)$ have been carried out, showing excellent radiolabelling properties. Quantitative complexation was achieved within 60 minutes under stoichiometric conditions, at room temperature and in the nanomolar concentration range. It was also demonstrated that the complexation occurred below pH = 2. Properties have been compared to those of the analogue bispidol bearing a N-methanecarboxylate substituent (**L_1**). Although both systems meet the required criteria to be used as new chelator for $^{64/67}Cu$ in terms of formation kinetic, thermodynamic stability, selectivity for Cu(II), kinetic inertness regarding redox or acid-assisted decomplexation processes, substitution of the carboxylic acid function by the phosphonic moiety is responsible for a significant increase of the thermodynamic stability of the Cu(II) complex (+ 2 log units for pCu) and also leads to an increase of the radiochemical yields with $^{64}Cu(II)$ which is quantitative for **L_2**.

Introduction

Bispidine derivatives are highly preorganized ligands that can accommodate metal ions with cis-octahedral, square pyramidal or pentagonal geometries.[1,2] They usually form thermodynamically very stable metal complexes with transition metal ions which often show high kinetic inertness.[3,4,5] Modification of the coordinating pendant arms can be used to tune the ligand denticity as well as all electronic, thermodynamic and kinetic parameters such as the ligand field, the metal selectivity, the stability constants and the redox potentials. Such properties are very appealing for applications in catalysis,[6,7,8,9,10,11,12] in molecular magnetism[13,14,15,16,17] and in nuclear medicine and diagnosis as chelator for $^{64/67}Cu$.[18,19,20,21]

This study focuses on the use of two bispidine derivatives (**L**$_1$, and **L**$_2$, Chart 1) as chelators for radioactive copper for application in immuno-Positron Emission Tomography (PET) (^{64}Cu, $t_{1/2}$ = 12.7 h, β^+, 17.8%, 653 keV, β^-, 38.4%, 579 keV).[22] In this context, bifunctional chelators (BFCs) are needed, providing a strong chelating site for radioactive copper complexation as well as a reactive function for conjugation to a monoclonal antibody (mAb) (or a fragment) of interest. Lots of progresses in antibody technologies as well as site-specific conjugation methods[23,24] have been made in the recent years and it is now within our grasp to find or design engineered mAb fragments for almost any molecular target.[25] Radiolabeled antibodies have been introduced in clinical use[26,27,28,29] and a large range of BFCs are now available.[30,31,32] However, only a few chelators fulfill all of the very specific criteria which are required to radiolabel antibody-BFC conjugates in good conditions, *i.e*. *(i)* fast radiolabelling (a few minutes to one hour) at room temperature and around physiological pH; *(ii)* high *in vivo* stability and kinetic inertness towards transmetallation, transchelation and reduction; and *(iii)* easy access synthesis and bio-conjugation.[33,34]

Chart 1. Structure of acid functionalized ligands (**L**$_1$-**L**$_2$) studied and the related bispidone (**L**$_3$).

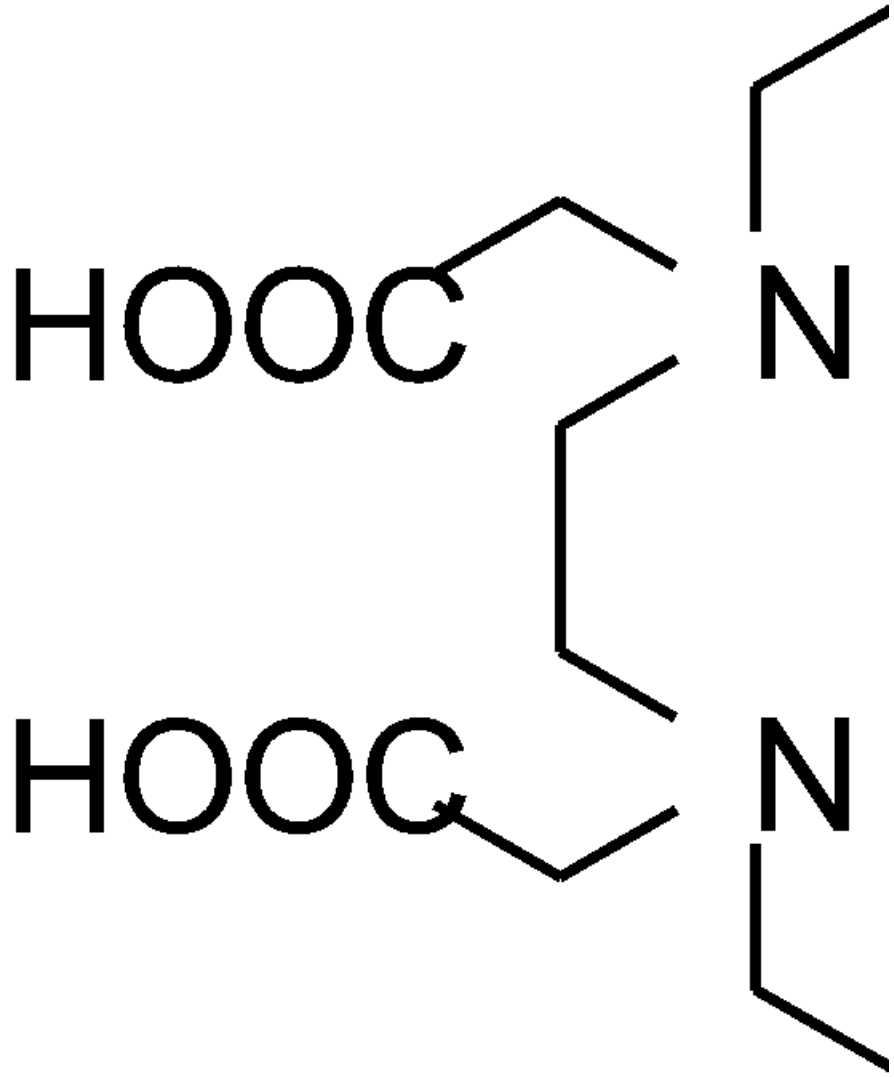


Chart 2. Structure of other ligands discussed in this work.

Three classes of ligands with polyaza donor sets are commonly used: macrocyclic, linear and macrobicyclic. NOTA[35,36] and TETA[37,38,39] and their derivatives are easily accessible but often

suffer from low kinetic inertness. Variations of the substituent are being explored in order to improve the *in vivo* stability of the Cu complexes (see HTE1PA,[40,41,42,43] NO1PA2PY[44] and its derivatives,[45] Chart 2). Very stable and inert cyclen-based cross-bridged systems (such as PycupBn[46] and CB-TE2A,[47] Chart 2) and macrobicycles such as **L_7**[48] are being developed but their slow kinetic of complexation is hampering their use for the labeling of antibodies. Faster complexation is observed with N-phosphonic acid analogues, although heating is still necessary for the moment.[49,50,51,52] New linear systems such as H_2DEDPA and H2AZAPA[53,54] as well as other type of macrocyclic ligands and cages (DiamSar[55,56,57] and its derivatives) offer good radiolabelling conditions at room temperature (Chart 2) and for some of them, a high degree of kinetic inertness. Bispidine derivatives (**L_4** and **L_5**, Chart 2) also form particularly stable Cu(II) complexes *in vitro* and *in vivo*. **L_4** and **L_5** could be radiolabeled with >95% radiolabelling yields within a minute at room temperature.[18,4] Non-optimized specific activities of less than 0.1 GBq/µmol were used for **L_4**[18] and **L_5**[19] and a specific activity of 26 GBq/µmol was obtained for **L_6** after 90 min at 50°C.[20] Preliminary *in vivo* studies in mice and rats for **L_4** and **L_6** indicated rapid blood and tissue clearance as well as the absence of demetallation. However, changes were observed over time in the radio-HPLC chromatogram of **L_4**, which were attributed to partial or total hydrolysis of the ester functions by the esterase in rat plasma.[18] Dioxotetraaza macrocycles (**L_6**, Chart 2) are also very stable, although efficient labeling was observed only after heating the samples at 50°C.[20]

Our previous studies on the methylene carboxylate-substituted bispidine **L_1**, have shown that this ligand is another good candidate for PET applications.[21] Fast complexation occurs even at low pH values (pH = 1), with a high binding constant for Cu(II) versus competing metals (Co(II), Ni(II), Zn(II)) and the complex is characterized by a strong stability in acidic medium ($t_{1/2}$ =

110 days at 25°C, 5M $HClO_4$) and upon reduction ($E_{1/2}$ = -430 mV *vs* NHE). Radiolabelling with $^{64}CuCl_2$ is fast (<5min) and easily performed at room temperature and at micromolar concentrations of **L_1** in water ($4 \leq pH \leq 6$).[58] In these conditions, ≥ 90% radiolabeling yields were obtained. Moreover, the risk of enzymatic degradation is suppressed since the ester functions have been hydrolyzed prior complexation. In this study, we report the synthesis and physicochemical evaluation and the radiolabelling studies of a new methane phosphonate analogue **L_2** in water. Substitution of the acetic acid pendant arm by a methanephosphonic acid moiety was expected to improve the ligand selectivity for Cu(II) and to increase the thermodynamic and kinetic stability of the complex. This expectation is corroborated by literature data on phosphonate pendant-armed tetraazamacrocyclic chelators such as PCB-TEA1P[51,59] as well as on the podal pyridine derivatives developed in our group, L_8 (Chart 2).[60,61,62]

	Radiolabelling conditions	**$t_{1/2}$**	**pCu[a]**	**E_{red} (mV *vs* NHE)**
TETA[31,32]	25°C, 60 min, pH 5-7	3.5 d (5M HCl, 30°C)	15.1	-980 (irrev)
CB-TE2A[51]	95°C, 60 min, pH 6-7	154 h (5M HCl, 90°C)	-	-880 ($E_{1/2}$)
HTE1PA[40,41]	r.t., 15 min, pH 5	32 min (HCl 1M, 25°C)	18.64	-
		144 min (5M $HClO_4$, 25°C)		
CB-TE1PA[94]	-	96 d (5M HClO4, 25°C)	16.6	-620 ($E_{1/2}$)
PCTA[63,35]	25°C, 5 min, pH 5.5	-	19.1	-
DiamSar[55,56,57]	25°C, 5-30 min, pH 5.5	40 h (5M HCl, 90°C)	-	-900 (irrev)
NOTA[30,64,32]	25°C, 30-60 min, pH 5.5-6.5	< 3 min (5M HCl, 30°C)	18.4	-700 (irrev)
NO1PA2PY[44]	r.t., 30 min, pH 6-7	204 min (3M, HCl, 90°C)	17.75	-518
H2DEDPA[53]	25°C, 5-10 min, pH 5.5	< 5 min (6M HCl, 90°C)	18.5	-920 (irrev)
H2AZAPA[65]	25°C, 5-10 min, pH 5.5	-	-	-

L_1[b,21]	r.t., 15 min, pH 2-6	110 d (5M $HClO_4$, 25°C)	17.0	-560
L_2[b]	r.t., 5-15 min, pH 3-6.6	> 20 months (5M $HClO_4$, 25°C)	19.1	-600
L_4[18,4]	r.t., 1 min, pH 6.5		16.28	-303
L_5[19]	r.t., 1 min, pH 5.5	-	-	-
L_6[20]	50°C, 60 min, pH 6.5	-	-	-
PCB-TEA1P[51]	60°C, 1h, pH 8	8d (12M HCl, 90°C)	-	-573
L_7[60,62]	-	-	15.5	-

[a]pCu = - log[$Cu(II)_{free}$], [Cu] = 10^{-6} M, [L] = 10^{-5} M, pH = 7.4
[b]This work.

Table 1. Radiolabelling conditions (at r.t.), half life ($t_{1/2}$), pCu and reduction potential (E_{red}) for a selection of ligands.

General Methods. Solvents and starting materials were purchased from Aldrich, Acros and Alfa Aesar and used without further purification. IR spectra were recorded on a Perkin Elmer Spectrum One Spectrophotometer as solid samples and only the most significant absorption bands are given in cm^{-1}. Elemental analyses and mass spectrometry analysis were carried out by the Service Commun d'Analyses of the University of Strasbourg. ^{1}H and ^{13}C NMR spectra and 2D COSY, NOESY, HSQC, and HMBC experiments were recorded on Bruker Avance 300 and Avance 400 spectrometers operating at 300 and 400 MHz, respectively. Chemical shifts are reported in ppm, relative to residual protonated solvent as internal reference.[66] The pH values given are corrected for the deuterium isotopic effects.[67] Elemental analysis and monoisotopic masses were calculated with the chemcalc software.[68]

X-ray Crystallography. Crystals of the intermediate **2** (Scheme 1) and **L_2** ligand suitable for X-ray diffraction were obtained by slow evaporation of methanol solutions. The crystals were placed in oil, and a single crystal was selected, mounted on a nylon loop and placed in a low-

temperature N_2 stream. X-Ray diffraction data collection was carried out on a Bruker APEX II Kappa-CCD diffractometer equipped with an Oxford Cryosystem liquid N_2 device, using Mo-Kα radiation (λ = 0.71073 Å) at 150(2) K (Centre de diffractométrie X, Université de Rennes 1, France). Bruker SMART program were used to refine the values of the cell parameters. Data reduction and correction for absorption (SADABS) were carried out using the Bruker SAINT programs. The structures were solved by direct methods using the SIR97 program,[69] and then refined with full-matrix least-square methods based on F^2 (SHELX-97)[70] with the aid of the WINGX program.[71] All non-hydrogen atoms were refined with anisotropic atomic displacement parameters.

For **2**, all H atoms were included in their calculated positions, whereas, for $\mathbf{L_2}$, H atoms carried by heteroatoms were refined with isotropic atomic displacement parameters. Crystallographic data for structural analysis of **2** and $\mathbf{L_2}$ ligand have been deposited with the Cambridge Crystallographic Data Centre under CCDC N° 1530206 and 1530205, respectively. Copies of this information may be obtained free of charge from the web site www.ccdc.cam.ac.uk.

Synthesis of the ligands. Piperidinone dimethyl-1-methyl-4-oxo-2,6-di(pyridin-2-yl)piperidine-3,5-dicarboxylate ($\mathbf{P_1}$) was synthesized according to previously reported procedure.[72]

(aminomethyl)phosphonic acid **1**. **1** was obtained in three steps from diethyl phosphate according to the Kabachnik-Fields reaction, according to an adaptation of the procedure used in reference.[73] (i) To a solution of diethylphosphite (3.27 mL, 94%, 20.7 mmol, 1.2 eq) in THF (9 mL) were successively added dibenzylamine (3.39 mL, 98%, 17.27 mmol, 1 eq) and formaldehyde (3.06 mL, 37% in water, 34.5 mmol, 2eq). The mixture was heated at 60°C under stirring for 24 h and the reaction was monitored by TLC. After completion of the reaction, the mixture was taken to

dryness under vacuum and the as-obtained yellow oil was dissolved in cyclohexane (60 mL) and washed with water (3 × 15 mL). Diethyl((dibenzylamino)methyl)phosphonate was obtained as a colorless oil after evaporation of the cyclohexane under reduced pressure (6 g, quantitative). ^{1}H NMR (400 MHz, $CDCl_3$): δ 1.19 (t, J = 7.1 Hz, 6H, CH_2CH_3), 2.77 (d, J = 10.5 Hz, 2H, NCH_2P), 3.67 (s, 4H, $NCH_2\Phi$), 3.95 (qd, J_1 = 7.1 Hz, J_2 = 7.5 Hz, 4H, CH_2CH_3), 7.11-7.28 (m, 10H, Φ). ^{31}P NMR (162 MHz, $CDCl_3$): δ = 25.7.

(ii) Palladium over charcoal (10%, 600 mg) was added to a solution of diethyl((dibenzylamino)methyl)phosphonate (6 g, 17.27 mmol) in EtOH (300 mL) and the mixture was refluxed under a flow of hydrogen for 24h. The crude mixture was filtrated on a sintered-glass filter funnel filled with celite and the solvent was removed under vacuum to yield diethyl(aminomethyl)phosphonate (4.8 g, quantitative). ^{1}H NMR (400 MHz, $CDCl_3$): δ 1.25 (t, J = 6.7 Hz, 6H, CH_2CH_3), 1.97 (s, 2H, NH_2), 2.94 (d, J = 10.2 Hz, 2H, NCH_2P), 4.05 (m, 4H, CH_2CH_3). ^{31}P NMR (162 MHz, $CDCl_3$): δ 27.35 ppm (qd, J_1 = 8.5 Hz, J_2 = 9.2 Hz).

(iii) diethyl(aminomethyl)phosphonate (4.81 g, 28.8 mmol) was dissolved in 6M hydrochloric acid (300 mL) and the mixture was refluxed for 16 h under stirring. After evaporation to dryness under reduced pressure, (aminomethyl)phosphonic acid **1** was obtained as a white powder (4.25 g, quantitative). ^{1}H NMR (400 MHz, $CDCl_3$) : δ 3.00 (d, J = 13.0 Hz, 2H). ^{31}P NMR (162 MHz, $CDCl_3$): δ 12.18 ppm.

*Bispidone **2***. (aminomethyl)phosphonic acid **1** (126 mg, 1.13 mmol, 1.1 eq) was dissolved in a H_2O/MeOH (3/7) mixture (11 ml) and stirred at room temperature in the presence of sodium hydrogenocarbonate (143 mg, 1.7 mmol, 1.7 eq). Piperidone $\mathbf{P_1}$ (396 mg, 1.0 mmol, 1 eq) in 8 ml of MeOH, was then added as well as formaldehyde (93.0 mg, 3.1 mmol, 3 eq, 0.23 ml, 37 % solution in H_2O). The reaction mixture was heated to 60°C for 5 h, the reaction being monitored

by TLC on (eluent: DCM/MeOH 9/1, R_f = 0.26). After completion of the reaction, the solvent was evaporated under reduced pressure and the crude product was suspended into EtOH (10 mL). Bispidone **2** was isolated by centrifugation as a white powder (187 mg, 35 %). ^{1}H NMR (400 MHz, CD_3OD): δ 1.87 (s, 3H, H3), 2.53 (d, J = 13.0 Hz, 2H, He), 3.15 (AB system, δ_A = 2.66, δ_B = 3.64, J_{AB} = 12.3 Hz, 4H, H6/H8), 3.72 (s, 6H, OCH_3), 4.68 (s, 2H, H2/H4), 7.35 (m, 2H, Hd), 7.42 (ddd, J_1 = 7.7 Hz, J_2 = 4.9 Hz, J_3 = 0.9 Hz, 2H, Hb), 7.84 (td, J_1 = 7.8 Hz, J_2 = 1.5 Hz, 2H, Hc), 8.83 (dd, 2H, Ha). ^{31}P NMR (162 MHz, CD_3OD): δ 15.29 ppm. ^{13}C NMR (100 MHz, CD_3OD): δ 41.9 (CH_3), 51.7 (2C, OCH_3), 57.2 (d, Ce), 60.9 (2C, C6), 63.0 (2C, C1), 72.4 (2C, C2), 123.8 (2C, Cb), 124.7 (2C, Cd), 137.6 (2C, Cc), 150.6 (2C, Ca), 156.3 (2C, Cpy), 167.5 (2C, CO_2Me), 202.3 (C9). Electrospray ionization (ESI) / MS^+ (CH_3OH): *m/z* = 519.17 ($[M+H]^+$, 100%). Anal. Calcd for $C_{23}H_{26}N_4O_8PNa\cdot 0.5H_2O$, C, 50.28, H, 4.95, N, 10.20. Found: C, 50.39, H, 4.75, N, 10.27.

*Bispidol **3***. Compound **2** (1.2 g, 2.3 mmol, 1 eq) was dissolved in 80 mL of anhydrous MeOH by heating and using ultrasound. The solution was then cooled to -78°C and sodium borohydride (107 mg, 2.8 mmol, 1.5 eq) was gradually added. The reaction was monitored by TLC on C18 (eluent: H_2O/ACN 7/3, R_f = 0.28). After 5h30, the reaction was quenched at -78°C by the addition of a saturated NH_4Cl aqueous solution (5 mL). The solvent was evaporated under vacuum and the crude product was purified by FPLC on a C18 reverse phase column (eluent system: H_2O/ACN 0.1 % TFA), giving the bispidol **3** (0.79 g, 66 %). ^{1}H NMR (400 MHz, CD_3OD): δ 1.74 (s, 3H, H3), 3.35 (d, J = 11 Hz, 2H, He), 3.62 (s, 6H, OCH_3), 4.0 (AB system, δ_A = 3.76, H6/8ax, δ_B = 4.23, H6/8eq, J = 12.7 Hz, 4H), 4.55 (s, 1H, H9), 4.98 (s, 2H, H2/H4), 7.43 (dd, J_1 = 7.0 Hz, J_2 = 5.2 Hz, 2H, Hb), 7.65 (d, J = 7.6 Hz, 2H, Hd), 7.87 (td, J_t = 7.7 Hz, J_d = 1.6 Hz, 2H, Hc), 8.74 (d, J = 4.1 Hz, 2H, Ha). ^{31}P NMR (162 MHz, CD_3OD): δ 8.24 ppm.

^{13}C NMR (100 MHz, CD_3OD): δ 40.7 (CH_3), 51.2 (2C, C1), 51.8 (2C, OCH_3), 53.2 (d, J = 133.9 Hz, Ce), 55.8 (2C, C6), 66.2 (2C, C2), 71.9 (C9), 123.9 (2C, Cb), 127.6 (2C, Cd), 137.4 (2C, Cc), 149.3 (2C, Ca), 155.5 (2C, Cpy), 168.7 (2C, CO_2Me). Electrospray ionization (ESI) / MS^+ (CH_3OH): *m/z* = 521.18 ($[M+H]^+$, 100%). Anal. Calcd for $C_{23}H_{29}N_4O_8P\cdot 0.5H_2O$, C, 52.17, H, 5.71, N, 10.58. Found: C, 51.94, H, 5.56, N, 10.41.

Ligand ***L*****$_2$**. Compound **3** (514 mg, 1 mmol, 1 eq) was dissolved in a THF/H_2O (1:1) mixture (30 mL) and a solution of sodium hydroxide (200 mg, 5 mmol, 5 eq) in water (5 mL) was added. The mixture was stirred at room temperature and the reaction was monitored by TLC (eluent system: H_2O/ACN 8:2, 0.1 % TFA, R*f* = 0.65). After completion of the reaction, the mixture was evaporated to dryness, redissolved in 1M hydrochloric acid and purified by flash chromatography with a C18 reverse phase column (eluent system: H_2O/ACN 0.1 % TFA), to give ligand **L$_2$**·NaCl·4H_2O (621 mg, quantitative). ^{1}H NMR (300 MHz, CD_3OD): δ 1.78 (s, 3H, NCH_3), 2.34 (d, J = 12.2 Hz, 2H, He), 2.67 (AB system, δ_A = 2.09, H6/8ax, δ_B = 3.24, H6/8eq, J_{AB} = 12.4 Hz, 4H), 3.88 (s, 1H, H9), 4.61 (s, 2H, H2/H4), 7.24 (m, 2H, Hb); 7.47 (d, J = 7.6 Hz, 2H, Hd), 7.65 (t, J = 7.3 Hz, Hc), 8.76 (d, J = 3.7 Hz, 2H, Ha). ^{31}P NMR (162 MHz, CD_3OD): δ 16.28 ppm (t, J = 12.0 Hz). ^{13}C NMR (100 MHz, CD_3OD): δ 42.9 (CH_3), 51.7 (2C, C1), 59.2 (2C, C6), 60.5 (d, J = 145.7 Hz, C9), 68.3 (2C, C2), 74.8 (C9), 122.0 (Cb), 125.7 (Cd), 136.1 (Cc), 149.5 (Ca), 160.62 (2C, Cpy), 178.34 (2C, CO_2H). Electrospray ionization (ESI) / MS^+ (CH_3OH): *m/z* = 493.15 $[M+H]^+$, 100%). Anal. Calcd for $C_{21}H_{25}N_4O_8P\cdot NaCl\cdot 4H_2O$, C, 40.49, H, 5.34, N, 8.99. Found: C, 40.32, H, 5.03, N, 8.92.

Physico-chemical studies.

Materials. Distilled water was purified by passing through a mixed bed of ion-exchanger (Bioblock Scientific R3-83002, M3-83006) and activated carbon (Bioblock Scientific ORC-83005). All the stock solutions were prepared by weighing solid products using an AG 245 Mettler Toledo analytical balance (precision 0.01 mg). Metal cation solutions were prepared from their perchlorate salts ($Cu(ClO_4)_2.6H_2O$, 98%, Fluka; $Zn(ClO_4)_2.6H_2O$, 98.9%, Alfa Aesar) and their concentrations were determined by colorimetric titrations with EDTA (10^{-2} M, Merck, Titriplex III) according to standard procedures.[74] Sodium hydroxyde (NaOH) and hydrochloric acid (HCl) were used to adjust pH during titrations. The ionic strength of all the solutions was fixed to 0.1 M with potassium chloride (KCl, Fluka, 99.0%). All the experiments described were repeated at least three times.

CAUTION! Perchlorate salts combined with organic ligands are potentially explosive and should be handled in small quantities and with the adequate precautions.[75]

Potentiometry. The protonated species of $\mathbf{L_2}$ and the stability constants of $\mathbf{L_2}$ complexes with Cu(II) and Zn(II) complexes were characterized and quantified by potentiometric titrations in water. All the solutions used in the potentiometric experiments were prepared from boiled and degassed water. Titrations were performed using an automated titrating system (DMS 716 Titrino, Metrohm) with a combined glass electrode (Metrohm, 6.0234.100, Long Life) filled with NaCl 0.1 M. The electrode was calibrated as a hydrogen concentration probe by titrating known amounts of hydrochloric acid with CO_3^{2-} free potassium hydroxide solutions. The GLEE program[76,77] was used for the glass electrode calibration.

In a typical experiment, an aliquot of 10 mL of $\mathbf{L_2}$ (2.10^{-3} M) or M:$\mathbf{L_2}$ (M = Cu(II) or Zn(II), [M]/[**L**] ≈ 1) was introduced into a thermostated jacketed cell (25.0(2) °C, Metrohm) and kept under argon during the titrations. The solutions were acidified with a known volume of HCl and the titrations were then carried out by addition of known volumes of potassium hydroxide solution over the pH range 2-12. The potentiometric data of $\mathbf{L_2}$ and its metal complexes were refined with the Hyperquad 2008 program[78] which uses non-linear least-squares methods, taking into account the formation of metal hydroxide species. The titration of each system was repeated at least in duplicate and the sets of data for each system were treated independently, then merged together and treated simultaneously to give the final stability constants. The distribution curves as a function of pH of the protonated species of $\mathbf{L_2}$ and of $\mathbf{L_2}$ metal complexes were calculated using the Hyss2009 program.[79]

Spectrophotometry. The protonation constants of $\mathbf{L_2}$ and the stability constants of M:$\mathbf{L_2}$ (M = Cu(II) and Zn(II) [M]/[**L**] ~ 1, [**L**] ~ 5.10^{-5} M) were also determined by UV-Visible spectrophotometric titration versus pH. Since complexation started in very acidic medium, the titrations were carried out in two different ways. Between pH = -0.6 and pH = 2, batch solutions were prepared. Each sample was prepared separately by mixing a known amount of $\mathbf{L_2}$ stock solution, a known amount of standardized $HClO_4$ to adjust the pH (pH = - log[H^+]) and a known amount of Cu(II) stock solution in the case of the study of the complexes ([Cu(II)]/[**L**) = 1). An absorption spectrum of each sample was recorded in a 1 cm quartz suprasil spectrophotometric cell using a Varian (Cary 3) UV-Visible spectrophotometer. Between pH 2 and 12.5, direct titrations were carried out. Typically, an aliquot of 10 mL of **L** solution was introduced into a thermostated jacketed titration vessel (25.0(2) °C) with 1 equivalent of metal (M) in the case of M:**L** titrations. A known volume of hydrochloric acid solution was added to adjust the pH around

2 and the titrations were carried out by addition of known volumes of potassium hydroxide solution. After each addition, the pH was allowed to equilibrate, an aliquot was transferred to a 1 cm quartz suprasil spectrophotometric cell, a spectrum was recorded using a Varian (Cary 3) spectrophotometer, the aliquot was transferred back to the titration vessel and a new addition was made. The free hydrogen ion concentrations were measured with a Mettler Toledo U402-S7/120 (pH 0-14) combined glass electrode. Potential differences were given by a Tacussel LPH430T millivoltmeter. Standardization of the millivoltmeter and verification of the linearity of the electrode were performed with three commercial buffer solutions (pH 4.01, 7.01 and 10.01, 25°C). The software Hypspec V1.1.33 was used to determine the coordination model and calculate the stability constants (log β) of the formed species. [71,80]

Acid decomplexation studies. Acid-decomplexation studies were performed under pseudo first-order conditions on two solutions of Cu$\mathbf{L_2}$ complex in 5 M $HClO_4$ at 25°C. Changes in the absorption spectra with time over a period of 20 months were monitored using a Perkin-Elmer Lambda 950 spectrophotometer. 1.98×10^{-4} mmol of Cu(II)$\mathbf{L_2}$ complex were used to monitor the π-π^* transition at 262 nm and 8.78×10^{-3} mmol to follow the d-d transition at 680 nm.

Cyclic voltammetry. Cyclic voltammetry (CV) was carried out on the Cu$\mathbf{L_2}$ complex at room temperature with a PC interfaced Radiometer Analytical MDE150/PST50. The CV experiments were performed using a glassy carbon working electrode (0.071 cm^2, BASi). The electrode surface was polished routinely with 0.05 μm alumina−water slurry on a felt surface immediately before use. The counter electrode was a Pt coil, and the reference electrode was a Ag/AgCl electrode. The Cu$\mathbf{L_2}$ complex was measured in Ar-degassed water with ionic strength fixed at 0.1M with $NaClO_4$ and the pH of the solutions were adjusted with NaOH and $HClO_4$ solutions.

Seven different values of pH (pH = 2.36, 4.04, 5.70, 7.2, 8.55, 10.23, 11.62) and different scan rates (50-300 mV/s) were considered

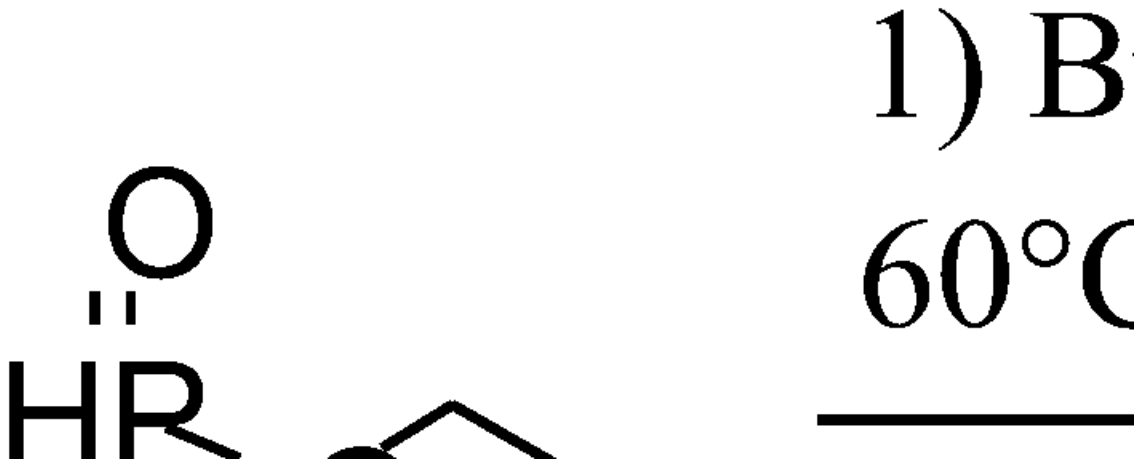
Radiolabelling.

$^{64}CuCl_2$ in 0.1M hydrochloric acid was obtained from the ARRONAX cyclotron (Saint-Herblain, France). Production and purification procedures have already been described.[81] Radiochemical purity was determined by gamma spectroscopy and chemical purity was measured by ICP-AES. Water (18.2 MΩ.cm) for aqueous solutions was obtained from a Milli-Q gradient system (Millipore). Radiolabelling of ligand $\mathbf{L_2}$ with ^{64}Cu was performed, following the same procedure than the one previously described for ligand $\mathbf{L_1}$.[58] Post-processed ^{64}Cu eluate diluted in 0.25 M ammonium acetate buffer (pH 5.3) were mixed at room temperature with a ligand stock solution ($[\mathbf{L_2}]_{stock}$ = 4.1 × 10^{-4} M). Four radionuclide batches were used for radiolabeling purposes. Each batch was characterized with regards to its specific activity (SA(^{64}Cu) per nmol of Cu) and the content of cold metallic impurities. Briefly, the characteristics of each batch (#1 to #4) is given : batch #1 (13.13 MBq/mL, $[Cu^{2+}]$ = 4.02 × 10^{-7} M, [M] = 2.48 × 10^{-5} M, SA(^{64}Cu) = 34.8 MBq/nmol), batch #2 (55.71 MBq/mL, $[Cu^{2+}]$ = 2.19 × 10^{-6} M, [M] = 8.93 × 10^{-6} M, SA(^{64}Cu) = 25.3 MBq/nmol), batch #3 (38.94 MBq/mL, $[Cu^{2+}]$ = 1.53 × 10^{-6} M, [M] = 8.94 × 10^{-6} M, SA(^{64}Cu) = 25.3 MBq/nmol), batch #4 (9.74 MBq/mL, $[Cu^{2+}]$ = 3.8 × 10^{-7} M, [M] = 8.94 × 10^{-6} M, SA(^{64}Cu) = 25.3 MBq/nmol). Several parameters were scrutinized in repeated experiments such as the pH of the reaction mixtures, the time and the ligand/metal molar ratio (where [metal] corresponds to the total concentration in metal salts, including non-radioactive contaminants from the source such as Co(II), Cu(II), Fe(II/III), Ni(II) and Zn(II)). In a typical experiments, 500 µL batch solutions were prepared separately by mixing a known amount of ^{64}Cu stock solution (5-40 µL, 0.5 MBq), a known volume of ligand stock solution and a known amount of $AcONH_4$

buffer, the pH being previously adjusted to the desired value ($2 \leq pH \leq 7$). The influence of temperature and incubation time on the reaction yield was also investigated on **L_2** for a L/M ratio of 0.25 by heating the samples for 1h at 80°C; the pH was measured before and after the heating. Radiolabelling was followed by spotting the reaction mixture onto a TLC Flex Plate (silica gel 60A, lF-254, 200 µm, Merck) followed by elution with conc. aq. NH_3/MeOH/H_2O 1/2/1 (v/v/v). Quantitative distribution of radioactivity on TLC plates was measured using an electronic autoradiography system (Cyclone, Perkin Elmer). Under these conditions the ^{64}Cu complexes (R_f = 0.9) and the free ^{64}Cu ($R_f < 0.1$) are well separated. All yields are given with the experimental uncertainties of the cyclone device of ±5%.

Results and Discussion.

Synthesis of ligand L_2.



Scheme 1. Synthesis of Ligand $\mathbf{L_2}$.

Ligand $\mathbf{L_2}$ was obtained in three steps from (aminomethyl)phosphonic acid **1** and the piperidinone precursor $\mathbf{P_1}$ following a similar synthetic strategy to that previously reported for the glycinate derivative $\mathbf{L_1}$ (Scheme 1).[21] **1** was quantitatively obtained by a Kabachnik-Fields reaction between diethyl phosphite, methanal and dibenzylamine. Hydrogenolysis of the benzyl protecting groups followed by acid hydrolysis of the diethyl ester moieties were performed by using standard conditions. Bispidone **2** was obtained in 35% by a double Mannich reaction between $\mathbf{P_1}$, **1** and methanal in the presence of $NaHCO_3$. By this method, pure bispidone **2** could be obtained by precipitation from ethanol. It can be noticed that previous attempts using diethyl(aminomethyl)phosphonate instead of the phosphonic acid lead to a mixture of products

which was difficult to purify by crystallizations or column chromatography. Selective reduction of the central ketone of **2** was achieved in good yield by addition of $NaBH_4$ in cold methanol (-78°C). A single epimer, with H_9 pointing toward N_7 was isolated after purification by reverse phase flash chromatography (FPLC) on a C18 column as evidenced by ^1H-^1H NOESY experiments. Interestingly, the same regioselectivity was previously observed with the acetate-substituted bispidol[21] suggesting a facial regioselectivity, which is probably due to the stabilization of the borohydride intermediate due to formation of hydrogen bonds with the carbonyl and the acid protons of the phosphonic or carboxylic acid on N_7 (see numbering on Scheme 1). Saponification of the methyl ester substituents was achieved at room temperature in presence of sodium hydroxide and the pure ligand could be isolated by reverse phase FPLC (see Supporting Information, Figures S1-S13 for the NMR spectra of **2**, **3** and $\mathbf{L_2}$).

Structural characterization of 2 and $\mathbf{L_2}$. Single crystals of **2** (as the sodium salt **2Na)** and $\mathbf{L_2}$ were obtained by slow evaporation of methanol solutions at room temperature. The crystal structure refinement confirms the chemical structure of **2** and ligand $\mathbf{L_2}$. The corresponding ORTEP view of the asymmetric unit is shown in Figure and 2, respectively and corresponding crystallographic data are presented in Tables 1 and 2.

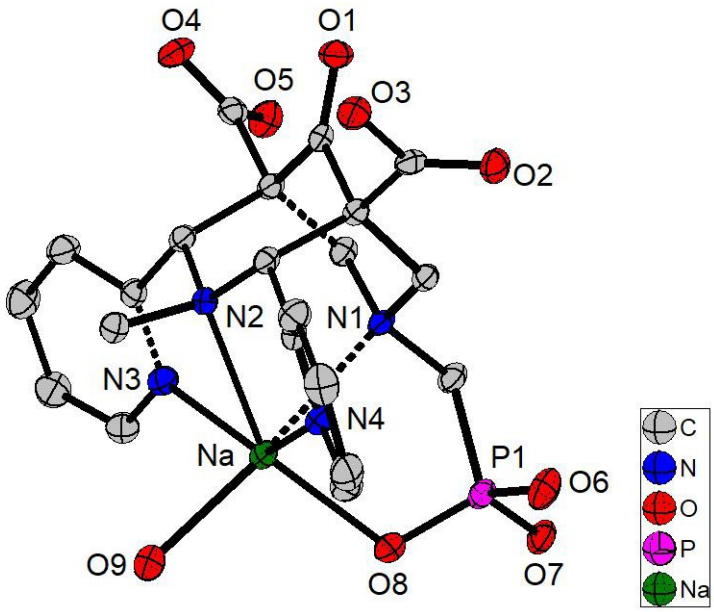


Figure 1. ORTEP drawing of **2Na** with the main atomic numbering. Thermal ellipsoids drawn at 50% probability level. All H atoms are omitted for the sake of clarity.

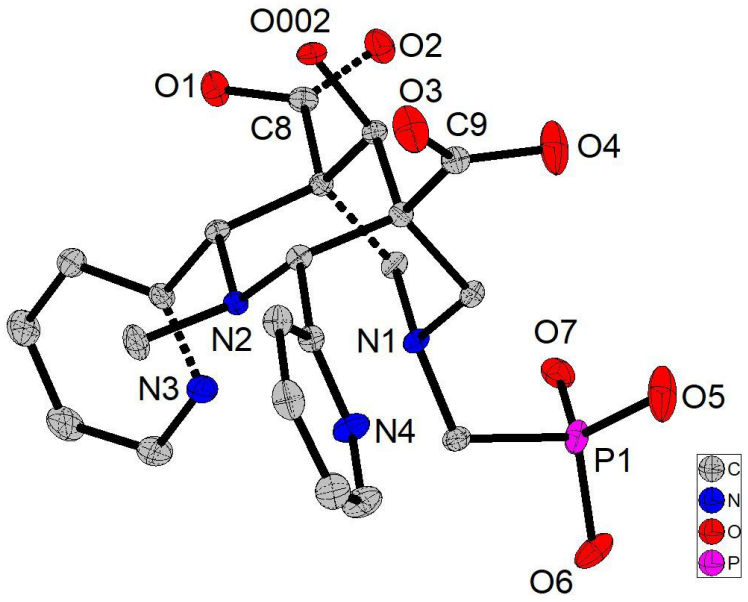


Figure 2. ORTEP drawing of ligand $\mathbf{L_2}$ with the main atomic numbering. Thermal ellipsoids drawn at 50% probability level. All H atoms are omitted for the sake of clarity.

Table 2**.** Crystallographic data for the structures of **2Na**, **L_2** and **L_3**.[72]

	2Na	**L_2**	**L_3**
Formula	$C_{24}H_{30}N_4NaO_9P$, MeOH	$C_{21}H_{25}N_4O_8P$, 2 MeOH	$C_{26}H_{30}N_4O_7$
Molecular weight ($g.mol^{-1}$)	604.52	556.50	510.54
Temperature (K)	150(2)	150(2)	173(2)
Crystal size (mm)	041 × 0.24 × 0.11	0.55 × 0.49 × 0.43	0.30 × 0.25 × 0.20
Crystal system	Triclinic	Monoclinic	Monoclinic
Space group	P-1	$P2_1/n$	$P2_1/c$
Unit-cell dim. (Å,°)	a= 8.3045(2) b= 13.5397(5) c= 14.3175(6) α= 113.495(2) β= 91.526(2) γ= 93.495(2)	a= 13.4531(5) b= 10.6527(3) c= 18.3216(7) β= 92.1580(10)	a= 14.8091(4) b= 11.8613(4) c= 14.8551(4) β= 100.775(2)
Volume ($Å^3$); Z	1471.37(9); 2	2623.84(16); 4	2563.37(13); 4
Density (calc.) ($g.cm^{-3}$)	1.364	1.409	1.323
Abs. coeff. (mm^{-1})	0.168	0.167	0.097
F(000)	636	1176	1080
θ_{max}	27.48	27.52	27.46
Reflections collected	14303	23378	25582
Independent reflections (I>2σ(I))	4964	5409	5860
Parameters	378	357	338
R1, wR2 (I>2σ(I))	0.0511, 0.1307	0.0367, 0.098	0.0566, 0.1418
R1, wR2 (all data)	0.0695, 0.1433	0.041, 0.1017	0.0832, 0.1555

Table 3. Selected Bond Lengths and Angles in **2**, **L_2** and **L_3**.[72]

	2	**L_2**	**L_3**
	Bond lengths and distances (Å)		
Na-N1	2.6205(18)		
Na-N2	2.4551(15)		
Na-N3	2.4802(23)		
Na-N4	2.4917(24)		

Na-O8	2.3330(15)		
Na-O9	2.3695(18)		
N1⋯N2	2.9429(24)	2.6935(13)	2.888(2)
N3⋯N4	4.6521(31)	4.6913(16)	7.186(2)
		Angles (deg)	
Pyr1⋯Pyr2	144.05	116.8	159.8

The intermediate **2** was isolated as a sodium salt and the structure (Figure 1) confirms the chair-chair conformation of the bispidone, as observed by ^{1}H NMR studies (Figure S1). This intermediate was crystallized in the triclinic P-1 space group with one sodium complex and one methanol molecule in general positions. The Na(I) ion is hexacoordinated by ligand **2** and one methanol molecule with a distorted octahedral coordination geometry (Table 2), which is, as expected from the strong rigidity of the ligand backbone, very similar to other hexacoordinated structures with Li(I)[82] or transition metal ions such as Cr(III), Mg(II), Fe(II), Co(II), Cu(I/II) or Zn(II).[5] In the case of **L_2**, the asymmetric unit contains one complete **L_2** ligand and 2 methanol molecules in general positions (Figure 2). The ligand crystallizes in a partially protonated form in the monoclinic space group $P2_1/n$ (Table 2) and is characterized by the presence of four acidic protons: one on the carboxylic acid (C9-O4H = 1.3150(16) and C9=O3 = 1.2035(16) Å), two on the phosphonic acid (P1=O5 = 1.4779(0), P1=O6H = 1.5598(10) and P1=O7H = 1.5616(10) Å) and a last one localized on the tertiary amine R_3NH^+ (N_2-H_2 = 0.894(17) Å). The carbon-oxygen distances on the remaining carboxylate are almost identical (C_8-O_1 = 1.2534(15) and C_8-O_2 1.2642(15) and the oxygen atoms O_1 and O_2 are involved in hydrogen bonds with a bidentate phosphonate of a neighboring molecule. Furthermore, the ammonium proton H_2 is stabilized inside the cavity by strong hydrogen bonds with the nitrogen atoms N_1 ($d_{H\text{-}N1}$ = 2.1142(105) Å), N_3 ($d_{H\text{-}N3}$ = 2.3543(78) Å) and N_4 ($d_{H\text{-}N4}$ = 2.5267(86) Å). Deeper analysis of the Fourier transform of the structure factors did not reveal any residual electron density around nitrogen

atom N1, meaning that in solid state, the proton is exclusively well-localized on the nitrogen atom N2. This protonation scheme is typical of a “proton sponge” behavior, which was confirmed by physicochemical titrations (see below). As a consequence, ligand **L_2** is highly preorganized for metal complexation with *(i)* a chair-chair conformation of the bispidine skeleton, *(ii)* a *cis*-symmetrical configuration of the pyridine rings and *(iii)* the lone pairs of N_1 and N_2 pointing towards the inside of the cavity. In addition, the $N_1\cdots N_2$ = 2.6935(13) and $N_3\cdots N_4$ = 4.6913(16) Å distances are significantly shorter than for analogous bispidone in their deprotonated form ($N_1\cdots N_2$ = 2.888(2) and $N_3\cdots N_4$ = 7.186(2) Å for **L_3**)[72] and very close to the distances measured for **2Na** and for another recent example of protonated structure with Hbispa ligands ($N_1\cdots N_2$ = 2.684(2) and $N_3\cdots N_4$ = 4.922(3) Å for Hbispa1a).[83] This contraction of the cavity is also likely attributed to the presence of the protonated ammonium center which more strongly attracts the electron-rich surrounding nitrogen atoms. Moreover, the structure is stabilized by a network of strong hydrogen bonds between the phosphonic acids and the acetate moiety of a neighboring molecule (O_1-O_6 = 2.5404(13) Å, O_1-H_{6A}-O_6 = 169.8(2)°, O_2-O_7 = 2.5632(13) Å, O_2-H_{7A}-O_7 = 177.8(2)° Å), which stabilizes this particular protonation state. Finally, each ligand form moderate H-bonds (O_2-O_8 = 2.8016(18) Å, O_2-H_8-O_8 = 157.2(1)°, O_9-O_{002} = 2.6677(16) Å, O_{002}-H_{002}-O_9 = 166.5(2)°) with two methanol molecules, the first one bridging the acetate group and the hydroxyl at C_9 and the second one being linked to the phosphonic acid. The rigid chair-chair conformation of the bicycle was also observed in solution by ^{1}H NMR (Figure S9) with typical Overhauser effect between the pyridyl protons H_d and the equatorial protons H_6 (see Figure S13 for ^{1}H-^{1}H NOESY). Attempts of growing single crystals of the CuL_2 complex have also been carried out unfortunately leading to crystals of insufficient quality for X-ray diffraction.

Thermodynamic Studies.

Protonation constants of ligand L_2.

Ligand **L_2** (Chart 1) has five protonable sites in the usual 2 ≤ pH ≤12 window in water: two tertiary amines, two carboxylic acids and one phosphonic acid. The crystal structure of **L_2** suggests that only one of two tertiary amines is protonated. However, three potential additional protonations constants have to be taken into account at lower pH values, which account for the second protonation of the phosphonic acid and for the protonations of the two pyridine rings.[21] Protonation constants, as defined by equations 1 and 2, were determined by a combination of potentiometric titrations (Figure S14) and UV–Visible absorption titrations versus pH between pH -0.6 and 12 (Figure 3).

$$LH_{n-1} + H \leftrightarrow LH_n \qquad (1)$$

$$K_n^H = \frac{[LH_n]}{[LH_{n-1}][H]} \quad n=1-6 \qquad (2)$$

Because of the known strong stability of the metal complexes of bispidine derivatives,[4,20] ligand **L_2** and its metal complexes were also studied in strongly acidic conditions (-0.59 < pH < 1.73) by means of spectrophotometric titrations *vs* pH. As such low pH cannot be measured with an electrode, the batch titration technique was used and the pH of the solutions was fixed by adding known volumes of standardized $HClO_4$ (see Experimental Section for details). It has to be noted that the ionic strength was not fixed below pH 1 in the batch titrations and that no decomposition of the ligand was observed, even in strongly acidic conditions. The spectral variations of **L_2** observed between -0.59 < pH < 1.73 (batch titration) and 2.10 < pH < 11.93 (direct titration)

were combined in Figure 3. $\mathbf{L_2}$ showed one band, centered at 263 nm, attributed to the π–π* transition of the pyridine rings, which underwent a hypochromic variation with the appearance of shoulders upon increase of the pH.[60] The hypochromic variation is typical of the deprotonation of pyridinium nitrogens while the shoulders appearing in basic conditions suggest the existence of hydrogen bonding with at least one pyridine nitrogen lone pair.[84]

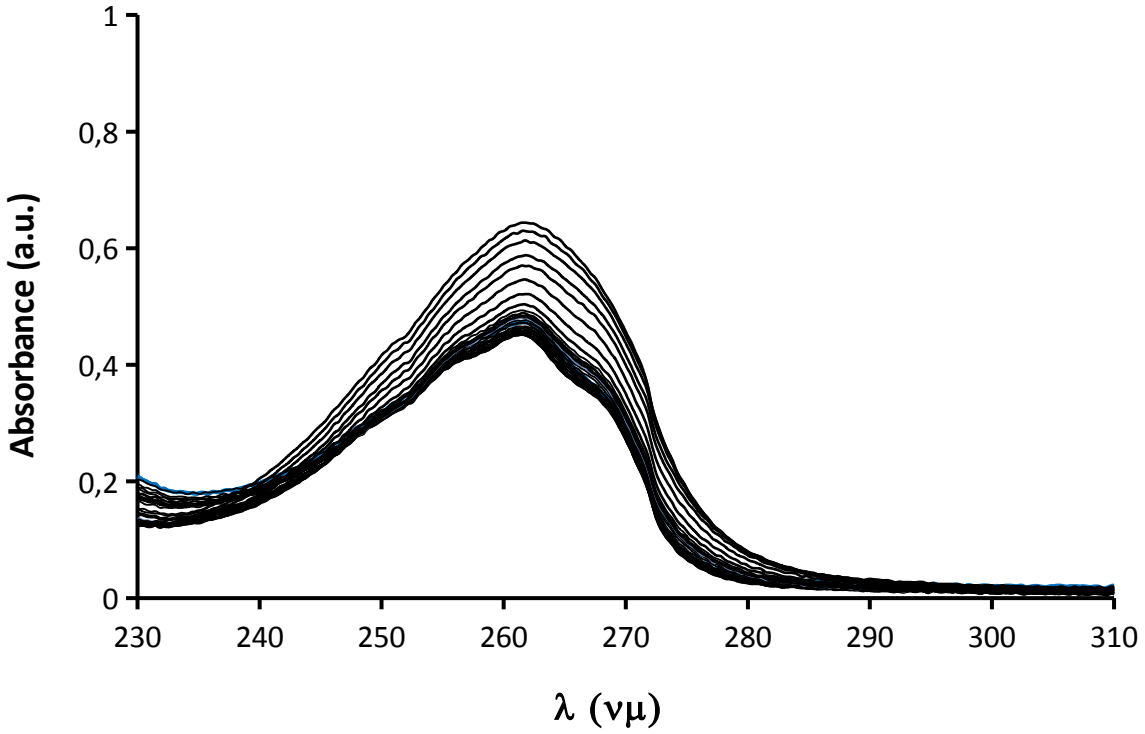


Figure 3. Spectrophotometric titrations of $\mathbf{L_2}$ vs pH between $-0.6 < p[H] < 1.73$ (Batch titration) and $2.10 \leq pH \leq 11.93$ (Direct titration). $[\mathbf{L_2}]_{tot} = 4.80 \times 10^{-5}$ M, Solvent: H_2O; I = 0.1 M KCl; T = 25.0(2) °C.

The statistical analysis of the potentiometric and spectrophotometric data versus pH was achieved with Hyperquad2008[85] and Hypspec softwares,[78] respectively, and led to the determination of five protonation constants of ligand $\mathbf{L_2}$ in the pH range from -0.59 to 11.93 (Table 4). The first protonation constant ($\log K_1^H$ =11.5(3)) was assigned to the tertiary amine of

the bispidine skeleton.[82,86,87,88] From crystallographic data, It was postulated that simultaneous protonation of the two tertiary amines does not occur. The second protonation constant (log K_2^H = 7.2(1)) was attributed to the first protonation of the phosphonic acid. The third and fourth protonation constants (K_3^H, K_4^H) were attributed to the two carboxylic acid oxygens. The two most acidic protonation constants belong to the pyridine nitrogens and/or to the second protonation of the phosphonic acid. Only one of them could be determined from our spectrophotometric batch titrations (log K_5^H = 0.5(1)). These protonation constants are in good agreement with those determined previously for ligand **L**[1] and for the analogue of **L₂** bearing a thiophene group in place of the phosphonic acid.[21]

Table 4. Successive Protonation Constants of **L₂** and **L₁**

pK_n^H		**L₂**	**L₁**
pK_1^H	N_{tert}	11.5(3)	10.6(6)
pK_2^H	HPO_3^-	7.2(1)	/
pK_3^H	COOH	3.8(3)	4.5(1)
pK_4^H	COOH	2.4(4)	2.0(2)
pK_5^H	PO_3^{2-}/ N_{pyr}	0.5(1)	0.82(1)
pK_6^H	N_{pyr}	<0.5	<0.82

H_2O, I = 0.1 M (KCl), T = 25.0 °C. The numbers in parentheses correspond to the standard deviations expressed as the last significant digit.

From these values, the electronic spectra of the protonated species of **L₂** (Figure 4a) and their distribution diagram (Figure 4b) were calculated.[89] The distribution curves showed that, due to the presence of the phosphonate moiety (pK_2^H = 7.2(1)), the ligand exists in its $\mathbf{L_2H^{3-}}$ and $\mathbf{L_2H_2^{2-}}$ forms under physiological conditions (pH 7.4).

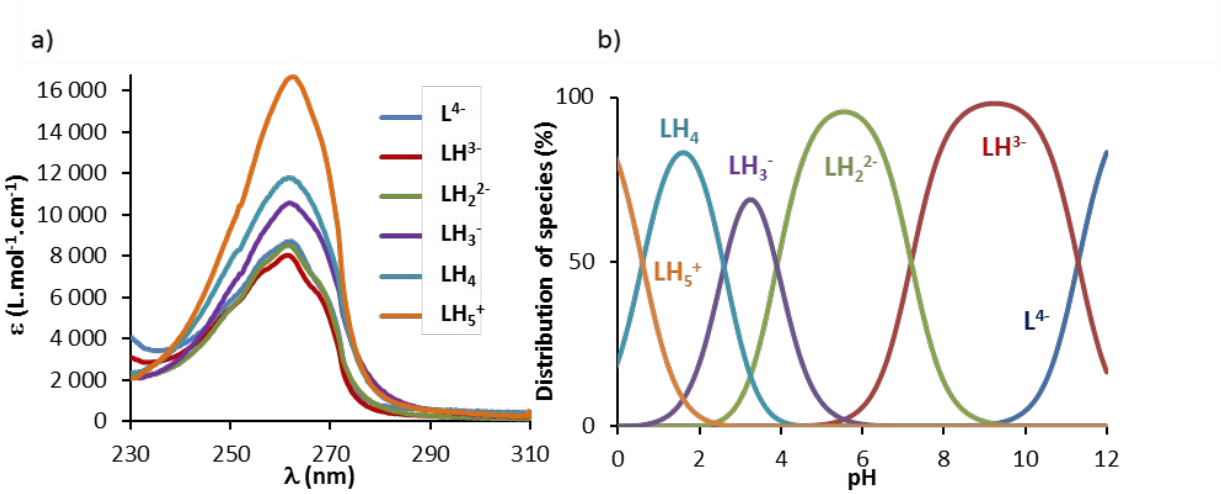


Figure 4. (a) Electronic spectra and (b) distribution diagram of the protonated species of $\mathbf{L}_2$ ($[\mathbf{L}_2]_{tot} = 5.0 \times 10^{-5}$ M, H_2O, $I = 0.1$ M KCl, $T = 25.0(2)$ °C).

Stability constants of the Cu(II) and Zn(II) complexes.

Spectrophotometric titrations versus pH of solutions of $\mathbf{L}_2$ and Cu(II) were carried out between pH = -0.59 and 2 (batch titration) to ensure complete decomplexation of Cu(II) and between pH = 2 and 12 (direct titration) both on the ligand bands and on the Cu(II) d–d bands (Figure 5). The position of the Cu(II) d–d bands at pH = 2 (λ_{max} = 682 nm) shows that the Cu(II) complex is already formed at this pH and suggests a square pyramidal geometry.[90] Significant changes were seen in the UV-visible absorption spectra of Cu$\mathbf{L}_2$ as a function of pH, where the hypo- and hypsochromic shift of the main band at 260 nm together with the appearance of a small charge transfer band (Figure 5a)[61] indicated the complete formation of the complex at pH = 0.2. Further spectral variations were observed between pH 2 and 12 suggesting the successive formation of different species.

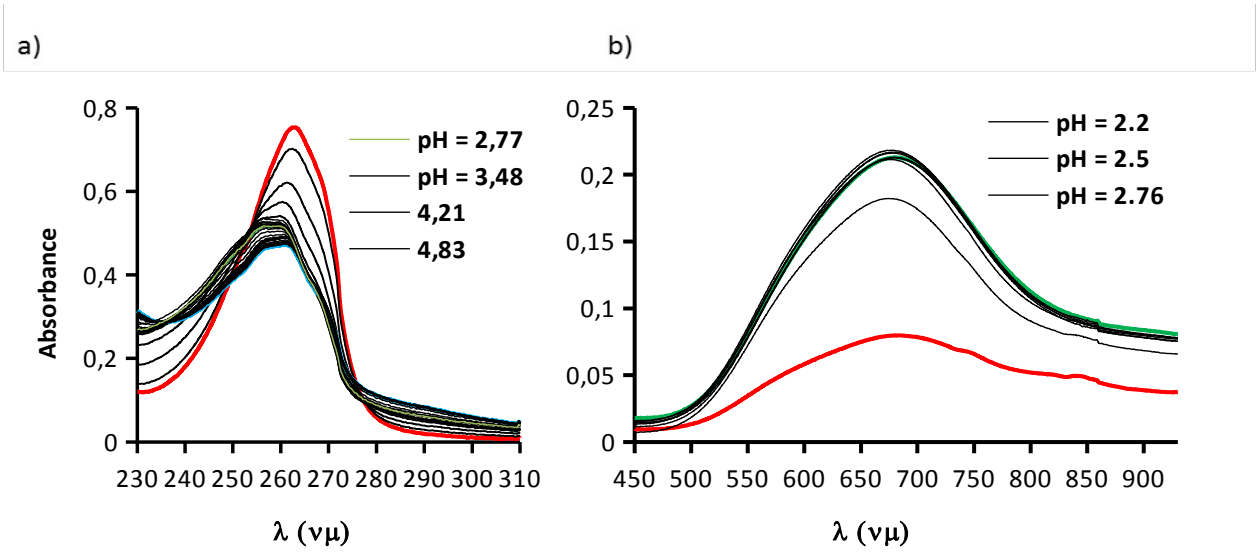


Figure 5. Spectrophotometric titration of Cu $\mathbf{L_2}$ vs pH: (a) $[\mathbf{L_2}]_{tot}$ = 4.79 × 10^{-5} M, $[Cu(II)]_{tot}$/ $[\mathbf{L_2}]_{tot}$ = 0.97, −0.60 < pH < 11.99, H_2O, I = 0.1 M (KCl), T = 25.0(2) °C.(b) $[\mathbf{L_2}]_{tot}$ = 2.50 × 10^{-3} M, $[Cu(II)]_{tot}$/$[\mathbf{L_2}]_{tot}$ = 0.97, −0.61 < pH < 12.07, H_2O, I = 0.1 M (KCl), T = 25.0(2).

Data analysis[85,78] suggested that the best model involves the successive formation of Cu$\mathbf{L_2}H_2$, Cu$\mathbf{L_2}$H and Cu$\mathbf{L_2}$ over the entire studied pH range (Table 5) with high stability constants. This model was confirmed by potentiometric titrations between pH 2-12 in which the Cu$\mathbf{L_2}H_2$ stability constant, determined from the batch titration, was fixed.

We then focused our attention on the study of the complexation of Zn(II) since it is a common metallic impurity in no-carrier-added radiocopper solutions.[81] Potentiometric and spectrophotometric titrations versus pH of $\mathbf{L_2}$ with stoichiometric amounts of Zn(II) showed the same model of complexation than for Cu(II), *i.e.* the successive formation of Zn$\mathbf{L_2}H_2$, Zn $\mathbf{L_2}$H and Zn$\mathbf{L_2}$ species.

Table 5. Overall Stability Constants (log β) of the M**L**$_2$ and M**L**$_1$ Complexes

	Cu(II)		Zn(II)	
	L$_1$	**L**$_2$	**L**$_1$	**L**$_2$
log β_{ML}	19.2(3)	22.5(1)	14.45(2)	18.8(1)
pKa_1		4.9(3)		5.3(2)
pKa_2		3.1(3)		3.1(2)
pM (pH 7.4)	17.0	19.1	12.2	15.4

[a] M = Cu(II), Zn(II), H_2O; I = 0.1M; T = 25.0°C, β_{MLH} = [MLH]/([M][L][H]); charges were omitted for clarity; log $K_{Cu(OH)}$ = −6.29; log $K_{Cu(OH)2}$ = −13.1; log $K_{Zn(OH)}$ = −7.89 ; log $K_{Zn(OH)2}$ = −14.92 (from ref 91). pM = −log[M(II)$_{free}$] with [M] = 10^{-6} M, [L] = 10^{-5} M, pH 7.4.

In order to compare the chelating ability of **L**$_2$ for Cu(II) and Zn(II) with other ligands, their pM (M = Cu(II), Zn(II)) values at physiological pH (pH 7.4) were calculated (Tables 1 and 5). By representing the amount of free metal in solution at physiological pH, the pM allows to compare the chelation power of ligands having different denticities and protonation properties for various metals. These results indicated a very strong stability of the Cu(II) complex bearing a phosphonate arm, with a pCu value two orders of magnitude larger than the previously studied ligand **L**$_1$ with a carboxylate arm and among the highest observed for ^{64}Cu PET ligands (Table 1). Moreover, ligand **L**$_2$ showed a good selectivity for Cu(II) compared to Zn(II), with more than 3 orders of magnitude increase in pM values between the Cu(II) and Zn(II) complexes.

The electronic spectra of the Cu(II) and Zn(II) complexes of **L**$_2$ (Figure 6a) and their species distribution profiles (Figure 6b) were calculated from their thermodynamic stability constants. The distribution curves show that for both Cu(II) and Zn(II), the M**L** complex is the major species at physiological pH (pH = 7.4).

a) b)

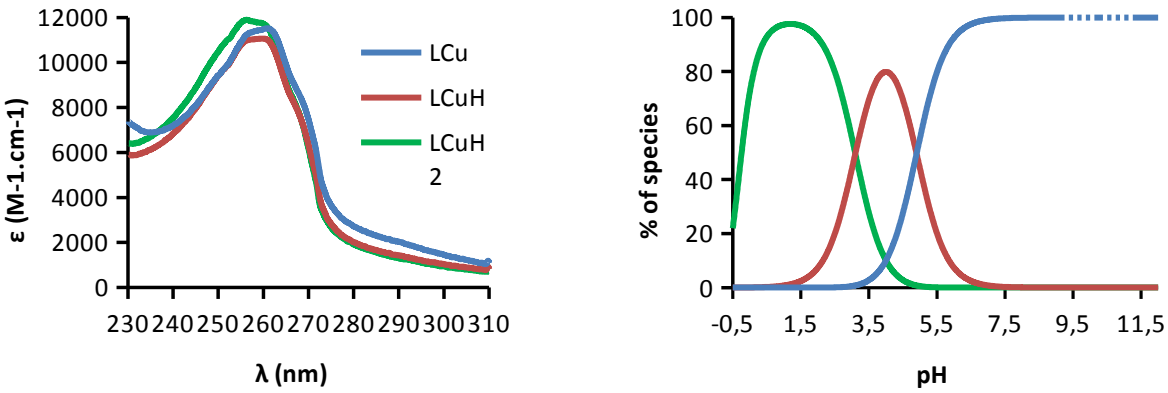


Figure 6. (a) Electronic spectra and (b) distribution diagram of the different Cu(II)-**L**$_2$ species ([**L**$_2$]$_{tot}$ = 5.05 × 10^{-5} M, [Cu]$_{tot}$/[L$_2$]$_{tot}$ = 0.98, H_2O, I = 0.1 M KCl, T = 25.0(2)°C).

pKas of the Zn(II) complexes have been confirmed by variable pH ^{1}H and ^{31}P NMR spectroscopy of a stoichiometric mixture of **L**$_2$ and $ZnCl_2$ in D_2O (Figure 7). At pD = 12.6, the ^{1}H NMR spectra is consistent with the formation of a rigid 1:1 complex (Figure S15) and all protons could be assigned by ^{1}H-^{1}H COSY and NOESY experiments (Figure S16). Significant variations are observed in the chemical shift of the protons $H_{6/8}$ ($\Delta\delta$ = 0.2 ppm), H_e ($\Delta\delta$ = 0.29 ppm), as well as of the phosphorus atom ($\Delta\delta$ = 4.63 ppm) (Figure 8, see numbering on Scheme 1). The strong variations on ^{31}P and on H_e suggest that the first protonation occurs on the phosphonate function and values of $pKa_{1(^{31}P)}$ = 5.4 and $pKa_{1(H6)}$ = 5.3 could be determined from the analysis of the chemical shift of the ^{31}P atom and proton H_6, respectively (Figure 7c). These results are in very good agreement with the pKa_1 obtained from potentiometric and spectrophotometric titrations. Protonation of the phosphonate also influences the chemical shift of the $H_{6/8}$ protons in the 4.8 ≤ pH ≤ 7.2 range. Moreover, the protonation curve of $H_{6/8}$eq clearly indicates that a second protonation reaction takes place below pH 4, which could be assigned to the protonation of a carboxylate function.

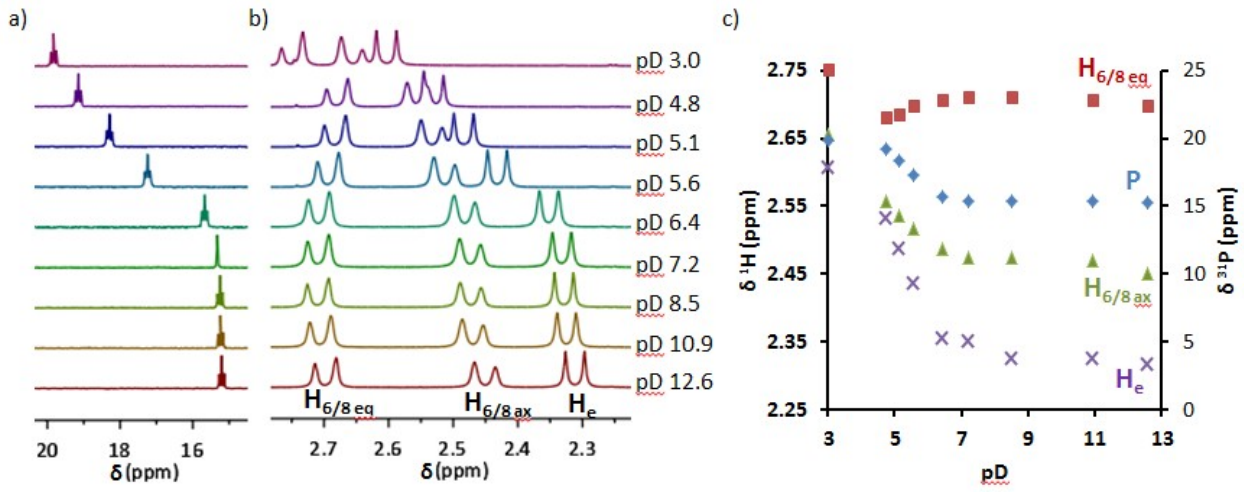


Figure 7. Variable pH NMR of a $\mathbf{L_2}$:$ZnCl_2$ 1:1 solution in D_2O at 25°C: (a) ^{31}P NMR spectra; (b) Zoom of the ^{1}H NMR spectra in the 2.25-2.75 ppm region; (c) Protonation curves = f(pD) for P, H_e, and $H_{6/8}$.

Electrochemical studies of the Cu(II) complexes with ligand $\mathbf{L_2}$.

In order to verify that the reduction potential of Cu$\mathbf{L_2}$ is below the threshold for *in vivo* reduction, estimated to -0.4V (vs NHE),[92,93] we performed cyclic voltammetry studies at different pH (Figure 8).

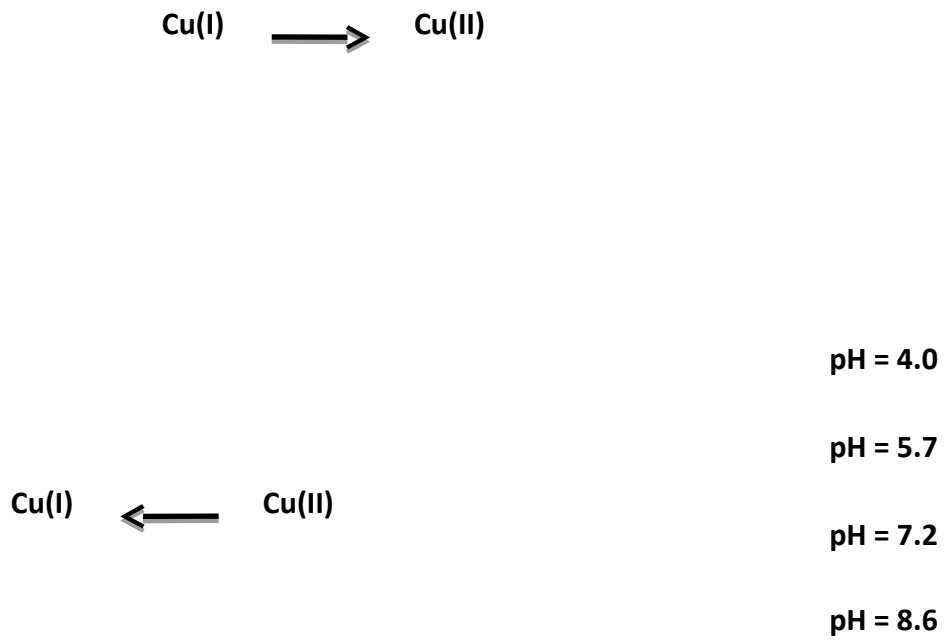


Figure 8. Cyclic voltammograms of Cu**L₂** at different pH (V = 200 mV/s). [Cu**L₂**] = 1.09 x 10^{-3} M, H_2O, I = 0.1 M ($NaClO_4$), T = 25.0(2)°C.

At physiological pH where the Cu**L₂** species predominates, quasi-reversible processes were observed both in reduction and oxidation. A single redox couple was identified, corresponding to Cu(II)/Cu(I) (E_{red} = −0.81 V vs Ag/AgCl *i.e.* E_{red} = −0.60 V vs NHE), clearly indicating the absence of demetallation and suggesting that **L₂** is able to stabilize both Cu(II) and Cu(I) in this pH range. Similar behaviors were also observed for ligand **L₁** and other bispidone derivatives [21,4] and for NO1PA2PY (E_{red} = −0.518 V *vs* NHE)[44] and CB-TE1PA ($E_{1/2}$ = -0.62 *vs* NHE).[94] Quasi-reversibility was also verified by measuring the peak anodic (i_{pa}) and cathodic (i_{pc}) currents with varying scan speed (v) at fixed pH. The linear plots of i_{pa} or $i_{pc} = f(v^{1/2})$ are shown in Figure S17. E_{red} is similar to the value obtained for ligand **L₁** (E_{red} = −0.56V), and is well below the estimated −0.40 V (*vs* NHE) threshold for typical bioreductants[30] and below Cu(II) complexes with bispidones **L₀** (E_{red} = −0.323 V *vs* NHE) and **HZ2** (E_{red} = −0.225 V *vs* NHE).[4] More stable

bispidine ligands have been reported more recently, however, redox potentials were measured in organic solvents such as DMF (E_{red} = − 1.17 V *vs* fc/fc+ *i.e.* E_{red} = -0.72 V *vs* NHE for [Cu(bispa[1b])]$^{+}$) and acetonitrile (E_{red} = -0.66 V *vs* fc/fc+ *i.e.* E_{red} = -0.26 V *vs* NHE for [Cu(N2py4)]$^{2+}$) and therefore cannot be compared with our system.[83] With such a low redox potential, the Cu**L₂** complex should not be subject to reduction, demetallation, or dismutation under physiological conditions. Below pH 5 and above pH 8.5 more complex phenomena were observed (Figure S18 in accordance with the distribution curves showing the presence of other chemical species.

Kinetic inertness of CuL_2H_2 in strongly Acidic Media.

Good candidates for radiopharmaceutical applications exhibit strong stability at physiological pH and in reductive medium, good selectivity, but more importantly, high kinetic inertness toward dissociation.[95] The kinetic inertness of a complex is commonly evaluated by following its acid-assisted dissociation in strongly acidic conditions under pseudo-first-order conditions. Providing all other criteria were satisfied, the obtained half-life was shown to be a good gauge of the in vivo stability of ^{64}Cu-labeled chelates.[96] The decomplexation of the Cu$\mathbf{L}_2H_2$ complex in 5 M $HClO_4$ aqueous solutions at 25 °C was followed by UV–visible absorption spectrophotometry both on the ligand π-π* transitions and the Cu(II) d-d bands over a period of 20 months. Very minor decomplexation is observed within the period, as assessed by the slight decrease of the absorption spectrum of the d-d transitions (only 6.4% at 670 nm, Figure S19), and which indicates a higher degree of inertness of the complex than the preciously studied Cu**L₁** ($t_{1/2}$ = 110 d) in the same conditions.

Radiolabelling studies.

The high stability of the Cu(II) complex prompted us to study the radiolabelling efficiency of ligand **L_2** with $^{64}CuCl_2$ in ammonium acetate buffer 0.1 M at room temperature. ^{64}Cu sources of different specific activities and cold metal impurities were used. For each experiment, the total concentration in metals ([M]) of the batch used is taken into account. Two series of measurements were performed in order to optimize the radiolabelling conditions. On the one hand, the influence of the ligand/metal ratio was investigated at a fixed pH of 5.4 and on the other hand, the influence of the pH (*i.e.* pH = 2 to 7) was studied for a fixed L/M ratio.

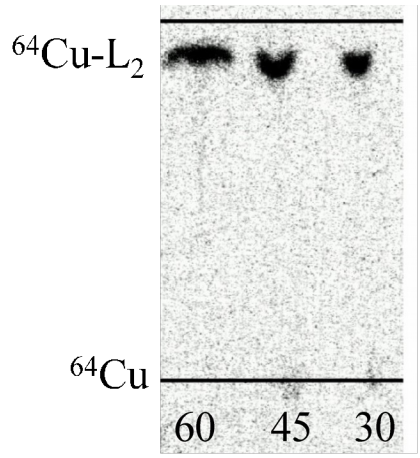


Figure 9. Thin layer radiochromatogram of ^{64}Cu-**L_2** after 30 min, 45 min and 60 min reaction time at pH 5.4 at r.t. in NH_4OAc 0.1 M (SiO_2, aq. NH_3/MeOH/H_2O 1/2/1).

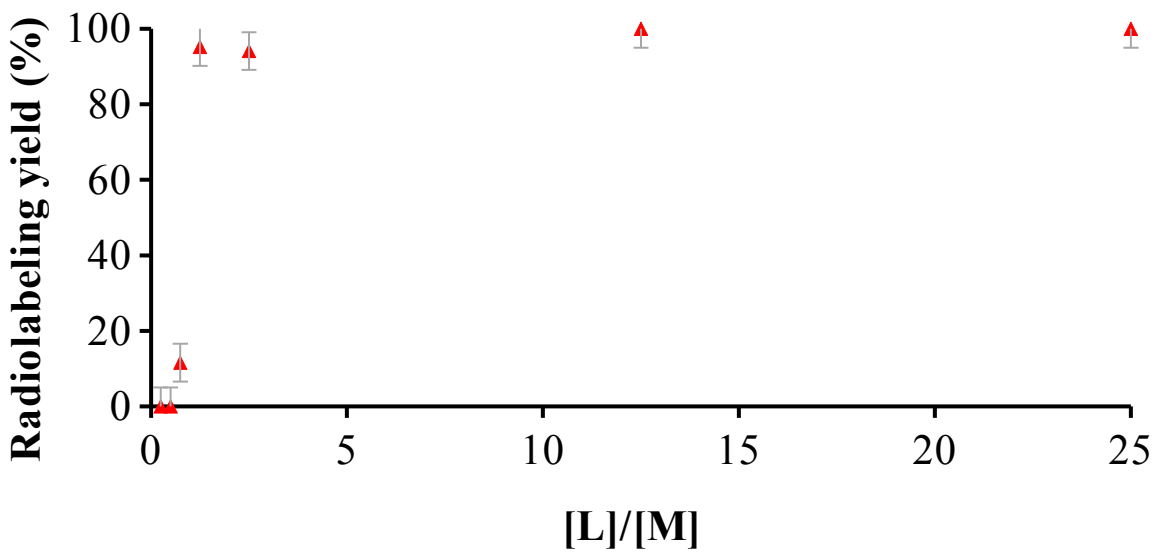


Figure 10. Radiolabelling yields of $\mathbf{L_2}$ (▲) at different ligand/metal ratios (NH_4OAc 0.1 M pH 5.4, r.t, 30 min, ^{64}Cu from batch 1, 0.12 nmol ≤ n(ligand) ≤ 12.0 nmol, n(Cu) = 8.04 pmol.

	t (min)					
L/M	5	10	15	30	45	60
0.25	0	0	0	0	0	0
0.5	0	0	0	0	0	0
0.75	0	0	0	12	11	11
1.25	≥ 95*	≥ 95*	≥ 95*	95	96	94
2.5	92	93	93	94	92	100
12.5	≥ 95*	≥ 95*	≥ 95*	100	100	100
25	100	100	100	100	100	100

Table 6. Time-dependence of the ^{64}Cu radiolabelling yields for $\mathbf{L_2}$ at different metal/ligand ratios (NH_4OAc 0.1 M pH 5.4, r.t., ^{64}Cu from batch 1, 0.12 nmol ≤ n(ligand) ≤ 12.0 nmol, n(Cu) = 8.04 pmol). *No free Cu(II) was seen on radio-TLCs.

Quantitative radiolabelling was achieved for ligand $\mathbf{L_2}$ after 30 min at room temperature with L/M ratios of 1.25 and above (Figure 9). In presence of sub-stoichiometric amount of ligand, radiolabelling did not occur at r.t. (Table 6). This might be explained by a slower kinetic of the

radiolabelling reaction, due to the presence of competitive metal salts (in particular Fe(II/III) was present at a concentration of 6.38 ppm in batch 1, which is relatively high for such production and purification processes). However, after incubation of the samples at 80°C for 1h, the ^{64}Cu-**L**$_2$ complex was formed in 4%, 5% and 22% yields for **L**$_2$/M ratios of 0.25, 0.5 and 0.75, respectively, at 80°C, which indicate a thermodynamic selectivity of **L**$_2$ for Cu(II) over the other cations. Moreover, very efficient radiolabelling (up to 95%) was achieved within 30 min at room temperature and with **L**$_2$/M ratios of only 1.25. In presence of a larger excess of ligand (25 equivalents), quantitative radiolabelling was achieved within 5 minutes only. In similar conditions, the radiochemical yield of ligand **L**$_1$ leveled at about 90%. In the case of **L**$_4$ and **L**$_5$ (Chart 2), radiochemical yields of 95% were obtained at room temperature in large excess of ligand (10^{-4}M). These results indicate a better radiolabelling capacity of the phosphonate derivative **L**$_2$ over the carboxylate and the pyridyl analogues, which is partly explained by the stronger thermodynamic stability of the copper(II) complex with **L**$_2$ (Table 6).

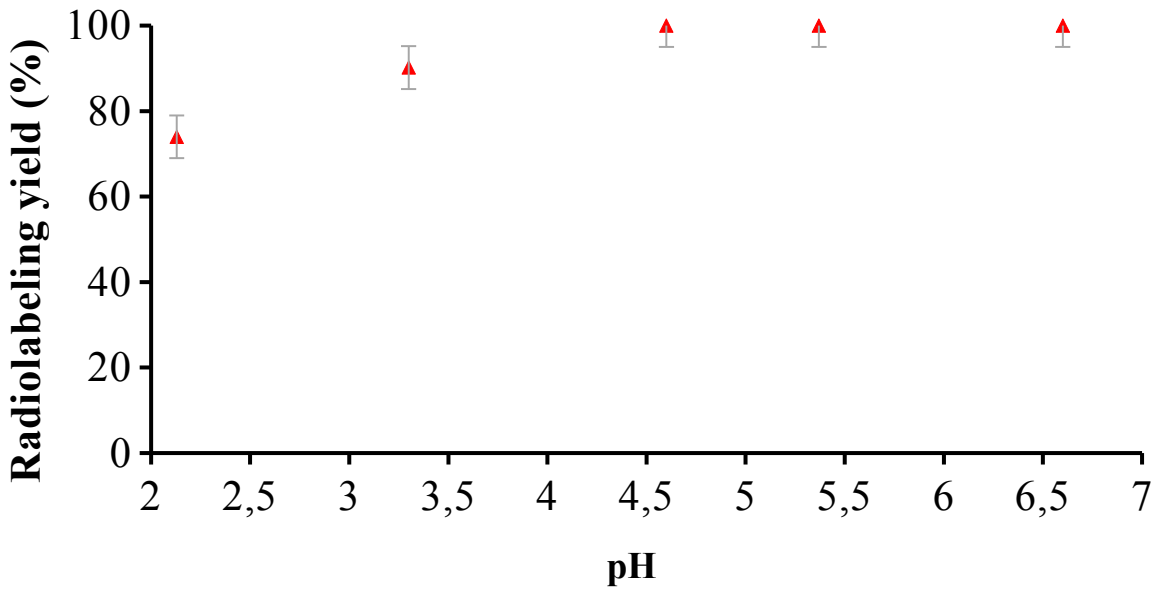


Figure 11. Radiolabelling yields of $\mathbf{L_2}$ (▲) at different pH values (r.t, NH_4OAc 0.1 M, 15 min, ^{64}Cu from batch 1 (pH 2.1 - 4.6), n(ligand) = 0.6 nm, n(Cu) = 8.04 pmol, and from batch 2 (pH 4.6-6.6), n(ligand) = 0.11 nmol, n(Cu) = 22.4 pmol, L/M = 1.25. *No free Cu(II) was seen on radio-TLCs. *No free Cu(II) was seen on radio-TLCs.

		t (min)					
	pH	5	10	15	30	45	60
$\mathbf{L_2}$	**2.1**	36	40	49	61	70	74
	3.3	60	70	-	87	89	90
	4.6	≥ 95*	≥ 95*	≥ 95*	-	-	-
	5.4	≥ 95*	≥ 95*	≥ 95*	95	96	94
	6.6	≥ 95*	≥ 95*	≥ 95*	100	100	100

Table 7. Time-dependence of the radiolabelling yields of $\mathbf{L_2}$ at different pH values (r.t, NH_4OAc 0.1 M, ^{64}Cu from batch 1 (pH 2.1 - 4.6), n(ligand) = 0.6 nm, n(Cu) = 8.04 pmol, and from batch 2 (pH 4.6-6.6), n(ligand) = 0.11 nmol, n(Cu) = 22.4 pmol, L/M = 1.25).

The influence of the pH was also investigated in the range 2.1-6.6 (Table 7, Figure 11). Results indicate that pH control is mandatory for ligand $\mathbf{L_2}$, the reaction kinetic being significantly slower in acidic conditions, probably due to the competition with the protonated species $\mathbf{L_2}H_3$, as

emphasized by potentiometric and X-ray crystallographic data. However, above pH 5.4, an efficient and quantitative radiolabelling was achieved at room temperature. With quantitative radiolabelling at ligand concentrations as low as 2×10^{-7} M, we believe that $\mathbf{L_2}$ is a promising system for the complexation of ^{64}Cu and that it is worth investigating its *in vivo* behavior in further studies.

Conclusion

In conclusion, the phosphonate pendant-armed bispidol ligand $\mathbf{L_2}$ was easily synthesized in three steps from piperidinone and (aminomethyl)phosphonic acid. The evaluation of the physico-chemical properties of the corresponding Cu(II) and Zn(II) complexes in water using UV-visible absorption spectrophotometry, potentiometry, ^{1}H and ^{31}P NMR, cyclic voltammetry as well as radiolabelling experiments with ^{64}Cu(II) has been reported. Fast complexation of Cu(II) occurs in the 4.6-6.6 pH range and the complex demonstrates a strong thermodynamic stability (log $\beta_{\mathrm{Cu}\mathbf{L}\mathbf{2}}$ = 22.5, pCu = 19.1 at pH 7.4), a good selectivity for Cu(II) *vs.* Zn(II) (pZn = 15.4 at pH 7.4), as well as a very good kinetic inertness regarding reduction (with a reversible redox potential of E_{red} = -0.60 vs NHE) and acid-assisted dissociation ($t_{1/2}$ >> 20 months). Quantitative radiolabelling (100% ± 5%) was achieved within 5 minutes at room temperature at pH above 5.4 at ligand concentrations as low as 2×10^{-7} M. From a coordination chemistry point of view, we believe that $\mathbf{L_2}$ meets all the required criteria to be used as new chelator for PET imaging with ^{64}Cu. Although it is out of the scope of the present paper, *in vitro* and *in vivo* stability studies as well as biodistribution studies are still needed to validate the potential of $\mathbf{L_2}$ for ^{64}Cu-immuno PET imaging. Several functionalization strategies are currently under study in order to obtain bifunctional ligands conjugated to antibodies.

ASSOCIATED CONTENT

Supporting Information. 1D and 2D NMR spectra, plots of potentiometric titration data, plot showing the influence of scan speed on current intensity at pH 7.4, cyclic voltammograms of CuL_2 at various pHs, plot of the evolution of the absorption spectra of the d-d transition on CuL_2H_2 in 5M $HClO_4$ over 20 months at 25°C and crystallographic data for 2Na and L_2 in CIF format. This material is available free of charge via the Internet at http://pubs.acs.org.

AUTHOR INFORMATION

Corresponding Author

*aline.nonat@unistra.fr, l.charbonn@unistra.fr. Give contact information for the author(s) to whom correspondence should be addressed.

Author Contributions

The manuscript was written through contributions of all authors. All authors have given approval to the final version of the manuscript.

ACKNOWLEDGMENT

This work was supported by the by the French Centre National de la Recherche Scientifique and the University of Strasbourg (UMR7178). The authors thank Mourad Elhabiri (Laboratoire de Chimie Médicinale et Bioorganique, UMR 7509 CNRS/UdS) for providing the facilities for cyclic voltammetry experiments as well as for thoughtful discussions. R. G. thanks the French Ministry of research and higher education for financial support for his PhD. The ARRONAX cyclotron is a project promoted by the Regional Council of Pays de la Loire, financed by local

authorities, the French government and the European Union. This work has been, in part, supported by the French National Agency for Research (“Investissements d’Avenir” research grant Equipex Arronax-Plus no. ANR-11-EQPX-0004 and Labex no. ANR-11-LABX-0018-01) and Labex IRON.

REFERENCES

(1) Comba, P.; Kerscher, M.; Schiek, W. Bispidine Coordination Chemistry. In *Progress in Inorganic Chemistry*; Karlin, K. D., Ed.; John Wiley & Sons, Inc., 2007; pp 613–704.

(2) Haller, R. Metal chelates of pyridyl-(2)-substituted 3,7-diaza-bicyclo-(3,3,1)-nonanones. *Arch. Pharm. Ber. Dtsch. Pharm. Ges.* **1969**, *302* (2), 113–118.

(3) Börzel, H.; Comba, P.; Hagen, K. S.; Lampeka, Y. D.; Lienke, A.; Linti, G.; Merz, M.; Pritzkow, H.; Tsymbal, L. V. Iron Coordination Chemistry with Tetra-, Penta- and Hexadentate Bispidine-Type Ligands. *Inorganica Chim. Acta* **2002**, *337*, 407–419.

(4) Born, K.; Comba, P.; Ferrari, R.; Lawrance, G. A.; Wadepohl, H. Stability Constants: A New Twist in Transition Metal Bispidine Chemistry. *Inorg. Chem.* **2007**, *46* (2), 458–464.

(5) Comba, P.; Kerscher, M.; Merz, M.; Müller, V.; Pritzkow, H.; Remenyi, R.; Schiek, W.; Xiong, Y. Structural Variation in Transition-Metal Bispidine Compounds. *Chem. – Eur. J.* **2002**, *8* (24), 5750–5760.

(6) Bukowski, M. R.; Comba, P.; Lienke, A.; Limberg, C.; Lopez de Laorden, C.; Mas-Ballesté, R.; Merz, M.; Que, L. Catalytic Epoxidation and 1,2-Dihydroxylation of Olefins with Bispidine–Iron(II)/H_2O_2 Systems. *Angew. Chem. Int. Ed.* **2006**, *45* (21), 3446–3449.

(7) Born, K.; Comba, P.; Daubinet, A.; Fuchs, A.; Wadepohl, H. Catecholase Activity of Dicopper(II)-Bispidine Complexes: Stabilities and Structures of Intermediates, Kinetics and Reaction Mechanism. *JBIC J. Biol. Inorg. Chem.* **2007**, *12* (1), 36–48.

(8) Comba, P.; Haaf, C.; Lienke, A.; Muruganantham, A.; Wadepohl, H. Synthesis, Structure, and Highly Efficient Copper-Catalyzed Aziridination with a Tetraaza-Bispidine Ligand. *Chem. – Eur. J.* **2009**, *15* (41), 10880–10887.

(9) Zayya, A. I.; Spencer, J. L. Coordination Chemistry of a Bicyclic 3-Aza-7-Phosphabicyclo[3.3.1]-Nonan-9-One Ligand. *Organometallics* **2012**, *31* (7), 2841–2853.

(10) Scharnagel, D.; Müller, A.; Prause, F.; Eck, M.; Goller, J.; Milius, W.; Breuning, M. The First Modular Route to Core-Chiral Bispidine Ligands and Their Application in Enantioselective Copper(II)-Catalyzed Henry Reactions. *Chem. – Eur. J.* **2015**, *21* (35), 12488–12500.

(11) Barman, P.; Vardhaman, A. K.; Martin, B.; Wörner, S. J.; Sastri, C. V.; Comba, P. Influence of Ligand Architecture on Oxidation Reactions by High-Valent Nonheme Manganese Oxo Complexes Using Water as a Source of Oxygen. *Angew. Chem. Int. Ed.* **2015**, *54* (7), 2095–2099.

(12) Ang, W. J.; Chng, Y. S.; Lam, Y. Fluorous Bispidine: A Bifunctional Reagent for Copper-Catalyzed Oxidation and Knoevenagel Condensation Reactions in Water. *RSC Adv.* **2015**, *5* (99), 81415–81428.

(13) Bautz, J.; Comba, P.; Que, L. Spin-Crossover in an Iron(III)−Bispidine−Alkylperoxide System. *Inorg. Chem.* **2006**, *45* (18), 7077–7082.

(14) Atanasov, M.; Busche, C.; Comba, P.; El Hallak, F.; Martin, B.; Rajaraman, G.; van Slageren, J.; Wadepohl, H. Trinuclear {M1}CN{M2}2 Complexes (M1 = CrIII, FeIII, CoIII; M2 = CuII, NiII, MnII). Are Single Molecule Magnets Predictable? *Inorg. Chem.* **2008**, *47* (18), 8112–8125.

(15) Atanasov, M.; Comba, P.; Helmle, S. Cyanide-Bridged FeIII–CuII Complexes: Jahn–Teller Isomerism and Its Influence on the Magnetic Properties. *Inorg. Chem.* **2012**, *51* (17), 9357–9368.

(16) Kolanowski, J. L.; Jeanneau, E.; Steinhoff, R.; Hasserodt, J. Bispidine Platform Grants Full Control over Magnetic State of Ferrous Chelates in Water. *Chem. – Eur. J.* **2013**, *19* (27), 8839–8849.

(17) Comba, P.; Rudolf, H.; Wadepohl, H. Synthesis and Transition Metal Coordination Chemistry of a Novel Hexadentate Bispidine Ligand. *Dalton Trans.* **2015**, *44* (6), 2724–2736.

(18) Juran, S.; Walther, M.; Stephan, H.; Bergmann, R.; Steinbach, J.; Kraus, W.; Emmerling, F.; Comba, P. Hexadentate Bispidine Derivatives as Versatile Bifunctional Chelate Agents for Copper(II) Radioisotopes. *Bioconjug. Chem.* **2009**, *20* (2), 347–359.

(19) Comba, P.; Hunoldt, S.; Morgen, M.; Pietzsch, J.; Stephan, H.; Wadepohl, H. Optimization of Pentadentate Bispidines as Bifunctional Chelators for ^{64}Cu Positron Emission Tomography (PET). *Inorg. Chem.* **2013**, *52* (14), 8131–8143.

(20) Comba, P.; Kubeil, M.; Pietzsch, J.; Rudolf, H.; Stephan, H.; Zarschler, K. Bispidine Dioxotetraaza Macrocycles: A New Class of Bispidines for 64Cu PET Imaging. *Inorg. Chem.* **2014**, *53* (13), 6698–6707.

(21) Roux, A.; Nonat, A. M.; Brandel, J.; Hubscher-Bruder, V.; Charbonnière, L. J. Kinetically Inert Bispidol-Based Cu(II) Chelate for Potential Application to 64/67Cu Nuclear Medicine and Diagnosis. *Inorg. Chem.* **2015**, *54* (9), 4431–4444.

(22) Brasse, D.; Nonat, A. Radiometals: Towards a New Success Story in Nuclear Imaging? *Dalton Trans.* **2015**, *44* (11), 4845–4858.

(23) Adumeau, P.; Sharma, S. K.; Brent, C.; Zeglis, B. M. Site-Specifically Labeled Immunoconjugates for Molecular Imaging—Part 1: Cysteine Residues and Glycans. *Mol. Imaging Biol.* **2016**, *18* (1), 1–17.

(24) Adumeau, P.; Sharma, S. K.; Brent, C.; Zeglis, B. M. Site-Specifically Labeled Immunoconjugates for Molecular Imaging—Part 2: Peptide Tags and Unnatural Amino Acids. *Mol. Imaging Biol.* **2016**, *18* (2), 153–165.

(25) England, C. G.; Hernandez, R.; Eddine, S. B. Z.; Cai, W. Molecular Imaging of Pancreatic Cancer with Antibodies. *Mol. Pharm.* **2016**, *13* (1), 8–24.

(26) Sehlin, D.; Fang, X. T.; Cato, L.; Antoni, G.; Lannfelt, L.; Syvänen, S. Antibody-Based PET Imaging of Amyloid Beta in Mouse Models of Alzheimer's Disease. *Nat. Commun.* **2016**, *7*, 10759.

(27) Wu, A. M. Antibodies and Antimatter: The Resurgence of Immuno-PET. *J. Nucl. Med.* **2009**, *50* (1), 2–5.

(28) Steiner, M.; Neri, D. Antibody-Radionuclide Conjugates for Cancer Therapy: Historical Considerations and New Trends. *Am. Assoc. Cancer Res.* **2011**, *17* (20), 6406–6416.

(29) Kaur, S.; Venktaraman, G.; Jain, M.; Senapati, S.; Garg, P. K.; Batra, S. K. Recent Trends in Antibody-Based Oncologic Imaging. *Cancer Lett.* **2012**, *315* (2), 97–111.

(30) Wadas, T. J.; Wong, E. H.; Weisman, G. R.; Anderson, C. J. Coordinating Radiometals of Copper, Gallium, Indium, Yttrium, and Zirconium for PET and SPECT Imaging of Disease. *Chem. Rev.* **2010**, *110* (5), 2858–2902.

(31) Shokeen, M.; Anderson, C. J. Molecular Imaging of Cancer with Copper-64 Radiopharmaceuticals and Positron Emission Tomography (PET). *Acc. Chem. Res.* **2009**, *42* (7), 832–841.

(32) Price, E. W.; Orvig, C. Matching Chelators to Radiometals for Radiopharmaceuticals. *Chem. Soc. Rev.* **2013**, *43* (1), 260–290.

(33) Price, T. W.; Greenman, J.; Stasiuk, G. J. Current Advances in Ligand Design for Inorganic Positron Emission Tomography Tracers Ga-68, Cu-64, Zr-89 and Sc-44. *Dalton Trans.* **2016**, *45* (40), 15702–15724.

(34) Bandara, N.; Sharma, A. K.; Krieger, S.; Schultz, J. W.; Han, B. H.; Rogers, B. E.; Mirica, L. M. Evaluation of ^{64}Cu-Based Radiopharmaceuticals That Target Aβ Peptide Aggregates as Diagnostic Tools for Alzheimer's Disease. *J. Am. Chem. Soc.* **2017**.

(35) Cooper, M. S.; Ma, M. T.; Sunassee, K.; Shaw, K. P.; Williams, J. D.; Paul, R. L.; Donnelly, P. S.; Blower, P. J. Comparison of ^{64}Cu-Complexing Bifunctional Chelators for Radioimmunoconjugation: Labeling Efficiency, Specific Activity, and in Vitro/in Vivo Stability. *Bioconjug. Chem.* **2012**, *23* (5), 1029–1039.

(36) Zhang, Y.; Hong, H.; Engle, J. W.; Bean, J.; Yang, Y.; Leigh, B. R.; Barnhart, T. E.; Cai, W. Positron Emission Tomography Imaging of CD105 Expression with a 64 Cu-Labeled Monoclonal Antibody: NOTA Is Superior to DOTA. *PLOS ONE* **2011**, *6* (12), e28005.

(37) Anderson, C. J.; Dehdashti, F.; Cutler, P. D.; Schwarz, S. W.; Laforest, R.; Bass, L. A.; Lewis, J. S.; McCarthy, D. W. ^{64}Cu-TETA-Octreotide as a PET Imaging Agent for Patients with Neuroendocrine Tumors. *J. Nucl. Med.* **2001**, *42* (2), 213–221.

(38) Pandya, D. N.; Kim, J. Y.; Park, J. C.; Lee, H.; Phapale, P. B.; Kwak, W.; Choi, T. H.; Cheon, G. J.; Yoon, Y.-R.; Yoo, J. Revival of TE2A; a Better Chelate for Cu(II) Ions than TETA? *Chem. Commun.* **2010**, *46* (20), 3517–3519.

(39) Pandya, D. N.; Bhatt, N.; Dale, A. V.; Kim, J. Y.; Lee, H.; Ha, Y. S.; Lee, J.-E.; An, G. I.; Yoo, J. New Bifunctional Chelator for 64Cu-Immuno-Positron Emission Tomography. *Bioconjug. Chem.* **2013**, *24* (8), 1356–1366.

(40) Lima, L. M. P.; Esteban-Gómez, D.; Delgado, R.; Platas-Iglesias, C.; Tripier, R. Monopicolinate Cyclen and Cyclam Derivatives for Stable Copper(II) Complexation. *Inorg. Chem.* **2012**, *51* (12), 6916–6927.

(41) Frindel, M.; Camus, N.; Rauscher, A.; Bourgeois, M.; Alliot, C.; Barré, L.; Gestin, J.-F.; Tripier, R.; Faivre-Chauvet, A. Radiolabeling of HTE1PA: A New Monopicolinate Cyclam Derivative for Cu-64 Phenotypic Imaging. In Vitro and in Vivo Stability Studies in Mice. *Nucl. Med. Biol.* **2014**, *41*, e49–e57.

(42) Frindel, M.; Camus, N.; Rauscher, A.; Bourgeois, M.; Alliot, C.; Barre, L.; Gestin, J.-F.; Tripier, R.; Faivre-Chauvet, A. Radiolabeling of HTE1PA: A New Monopicolinate Cyclam Derivative for Cu-64 Phenotypic Imaging. In Vitro and in Vivo Stability Studies in Mice. *Nucl. Med. Biol.* **2014**, *41 Suppl*, e49-57.

(43) Frindel, M.; Le Saëc, P.; Beyler, M.; Navarro, A.-S.; Saï-Maurel, C.; Alliot, C.; Chérel, M.; Gestin, J.-F.; Faivre-Chauvet, A.; Tripier, R. Cyclam Te1pa for ^{64} Cu PET Imaging. Bioconjugation to Antibody, Radiolabeling and Preclinical Application in Xenografted Colorectal Cancer. *RSC Adv* **2017**, *7* (15), 9272–9283.

(44) Roger, M.; Lima, L. M. P.; Frindel, M.; Platas-Iglesias, C.; Gestin, J.-F.; Delgado, R.; Patinec, V.; Tripier, R. Monopicolinate-Dipicolyl Derivative of Triazacyclononane for Stable Complexation of Cu^{2+} and $^{64}Cu^{2+}$. *Inorg. Chem.* **2013**, *52* (9), 5246–5259.

(45) Guillou, A.; Lima, L. M. P.; Roger, M.; Esteban-Gòmez, D.; Delgado, R.; Platas-Iglesias, C.; Patinec, V.; Tripier, R. 1,4,7-Triazacyclononane-Based Bifunctional Picolinate Ligands for Efficient Copper Complexation: 1,4,7-Triazacyclononane-Based Bifunctional Picolinate Ligands for Efficient Copper Complexation. *Eur. J. Inorg. Chem.* **2017**, *2017* (18), 2435–2443.

(46) Boros, E.; Rybak-Akimova, E.; Holland, J. P.; Rietz, T.; Rotile, N.; Blasi, F.; Day, H.; Latifi, R.; Caravan, P. Pycup? A Bifunctional, Cage-like Ligand for ^{64} Cu Radiolabeling. *Mol. Pharm.* **2014**, *11* (2), 617–629.

(47) Wadas, T. J.; Anderson, C. J. Radiolabeling of TETA- and CB-TE2A-Conjugated Peptides with Copper-64. *Nat. Protoc.* **2007**, *1* (6), 3062–3068.

(48) Esteves, C. V.; Lamosa, P.; Delgado, R.; Costa, J.; Désogère, P.; Rousselin, Y.; Goze, C.; Denat, F. Remarkable Inertness of Copper(II) Chelates of Cyclen-Based Macrobicycles with Two *Trans* - *N* -Acetate Arms. *Inorg. Chem.* **2013**, *52* (9), 5138–5153.

(49) Ferdani, R.; Stigers, D. J.; Fiamengo, A. L.; Wei, L.; Li, B. T. Y.; Golen, J. A.; Rheingold, A. L.; Weisman, G. R.; Wong, E. H.; Anderson, C. J. Synthesis, Cu(II) Complexation,

^{64}Cu-Labeling and Biological Evaluation of Cross-Bridged Cyclam Chelators with Phosphonate Pendant Arms. *Dalton Trans.* **2012**, *41* (7), 1938–1950.

(50) Zeng, D.; Ouyang, Q.; Cai, Z.; Xie, X.-Q.; Anderson, C. J. New Cross-Bridged Cyclam Derivative CB-TE1K1P, an Improved Bifunctional Chelator for Copper Radionuclides. *Chem. Commun.* **2013**, *50* (1), 43–45.

(51) Dale, A. V.; An, G. I.; Pandya, D. N.; Ha, Y. S.; Bhatt, N.; Soni, N.; Lee, H.; Ahn, H.; Sarkar, S.; Lee, W.; Huynh, P. T.; Kim, J. Y.; Gwon, M.-R.; Kim, S. H.; Park, J. G.; Yoon, Y.-R.; Yoo, J. Synthesis and Evaluation of New Generation Cross-Bridged Bifunctional Chelator for 64Cu Radiotracers. *Inorg. Chem.* **2015**, *54* (17), 8177–8186.

(52) Bhatt, N.; Soni, N.; Ha, Y. S.; Lee, W.; Pandya, D. N.; Sarkar, S.; Kim, J. Y.; Lee, H.; Kim, S. H.; An, G. I.; Yoo, J. Phosphonate Pendant Armed Propylene Cross-Bridged Cyclam: Synthesis and Evaluation as a Chelator for Cu-64. *Acs Med. Chem. Lett.* **2015**, *6* (11), 1162–1166.

(53) Boros, E.; Cawthray, J. F.; Ferreira, C. L.; Patrick, B. O.; Adam, M. J.; Orvig, C. Evaluation of the H2dedpa Scaffold and Its CRGDyK Conjugates for Labeling with 64Cu. *Inorg. Chem.* **2012**, *51* (11), 6279–6284.

(54) Ramogida, C. F.; Boros, E.; Patrick, B. O.; Zeisler, S. K.; Kumlin, J.; Adam, M. J.; Schaffer, P.; Orvig, C. Evaluation of H_2CHXdedpa, H_2Dedpa- and H_2CHXdedpa-N,N′-Propyl-2-NI Ligands for ^{64}Cu(II) Radiopharmaceuticals. *Dalton Trans* **2016**, *45* (33), 13082–13090.

(55) Di Bartolo, N.; Sargeson, A. M.; Smith, S. V. New Cu-64 PET Imaging Agents for Personalised Medicine and Drug Development Using the Hexa-Aza Cage, SarAr. *Org. Biomol. Chem.* **2006**, *4* (17), 3350–3357.

(56) Paterson, B. M.; Buncic, G.; McInnes, L. E.; Roselt, P.; Cullinane, C.; Binns, D. S.; Jeffery, C. M.; Price, R. I.; Hicks, R. J.; Donnelly, P. S. Bifunctional ^{64}Cu-Labelled Macrobicyclic Cage Amine Isothiocyanates for Immuno-Positron Emission Tomography. *Dalton Trans.* **2015**, *44* (11), 4901–4909.

(57) Bartolo, N. M. D.; Sargeson, A. M.; Donlevy, T. M.; Smith, S. V. Synthesis of a New Cage Ligand, SarAr, and Its Complexation with Selected Transition Metal Ions for Potential Use in Radioimaging. *J. Chem. Soc. Dalton Trans.* **2001**, No. 15, 2303–2309.

(58) Roux, A.; Gillet, R.; Huclier-Markai, S.; Ehret-Sabatier, L.; Charbonnière, L. J.; Nonat, A. M. Bifunctional Bispidine Derivatives for Copper-64 Labelling and Positron Emission Tomography. *Org. Biomol. Chem.* **2017**, *15* (6), 1475–1483.

(59) Lukeš, I.; Kotek, J.; Vojtíšek, P.; Hermann, P. Complexes of Tetraazacycles Bearing Methylphosphinic/Phosphonic Acid Pendant Arms with Copper(II), Zinc(II) and Lanthanides(III). A Comparison with Their Acetic Acid Analogues. *Coord. Chem. Rev.* **2001**, *216–217*, 287–312.

(60) Abada, S.; Lecointre, A.; Déchamps-Olivier, I.; Platas-Iglesias, C.; Christine, C.; Elhabiri, M.; Charbonniere, L. Highly Stable Acyclic Bifunctional Chelator for ^{64}Cu PET Imaging. *Radiochim. Acta* **2011**, *99* (10), 663–678.

(61) Abada, S.; Lecointre, A.; Christine, C.; Ehret-Sabatier, L.; Saupe, F.; Orend, G.; Brasse, D.; Ouadi, A.; Hussenet, T.; Laquerrière, P.; Elhabiri, M.; Charbonnière, L. J. Phosphonated Chelates for Nuclear Imaging. *Org. Biomol. Chem.* **2014**, *12* (47), 9601–9620.

(62) Abada, S.; Lecointre, A.; Elhabiri, M.; Charbonnière, L. J. Formation of Very Stable and Selective Cu(II) Complexes with a Non-Macrocyclic Ligand: Can Basicity Rival Pre-Organization? *Dalton Trans.* **2010**, *39* (38), 9055–9062.

(63) Ferreira, C. L.; Yapp, D. T.; Lamsa, E.; Gleave, M.; Bensimon, C.; Jurek, P.; Kiefer, G. E. Evaluation of Novel Bifunctional Chelates for the Development of Cu-64-Based Radiopharmaceuticals. *Nucl. Med. Biol.* **2008**, *35* (8), 875–882.

(64) Bevilacqua, A.; Gelb, R. I.; Hebard, W. B.; Zompa, L. J. Equilibrium and Thermodynamic Study of the Aqueous Complexation of 1,4,7-Triazacyclononane-N,N',N''-Triacetic Acid with Protons, Alkaline-Earth-Metal Cations, and Copper(II). *Inorg. Chem.* **1987**, *26* (16), 2699–2706.

(65) Bailey, G. A.; Price, E. W.; Zeglis, B. M.; Ferreira, C. L.; Boros, E.; Lacasse, M. J.; Patrick, B. O.; Lewis, J. S.; Adam, M. J.; Orvig, C. H2azapa: A Versatile Acyclic Multifunctional Chelator for ^{67}Ga, ^{64}Cu, ^{111}In, and ^{177}Lu. *Inorg. Chem.* **2012**, *51* (22), 12575–12589.

(66) Gottlieb, H. E.; Kotlyar, V.; Nudelman, A. NMR Chemical Shifts of Common Laboratory Solvents as Trace Impurities. *J. Org. Chem.* **1997**, *62* (21), 7512–7515.

(67) Mikkelsen, K.; Nielsen, S. O. Acidity Measurements with the Glass Electrode in H_2O-D_2O Mixtures. *J. Phys. Chem.* **1960**, *64* (5), 632–637.

(68) Patiny, L.; Borel, A. ChemCalc: A Building Block for Tomorrow's Chemical Infrastructure. *J. Chem. Inf. Model.* **2013**, *53* (5), 1223–1228.

(69) Altomare, A.; Burla, M. C.; Camalli, M.; Cascarano, G. L.; Giacovazzo, C.; Guagliardi, A.; Moliterni, A. G. G.; Polidori, G.; Spagna, R. SIR97: A New Tool for Crystal Structure Determination and Refinement. *J. Appl. Crystallogr.* **1999**, *32*, 115–119.

(70) Sheldrick, G. M. A Short History of SHELX. *Acta Crystallogr. Sect. A* **2008**, *64*, 112–122.

(71) Farrugia, L. J. WinGX Suite for Small-Molecule Single-Crystal Crystallography. *J. Appl. Cryst.* 1999, pp 837–839.

(72) Legdali, T.; Roux, A.; Platas-Iglesias, C.; Camerel, F.; Nonat, A. M.; Charbonnière, L. J. Substitution-Assisted Stereochemical Control of Bispidone-Based Ligands. *J. Org. Chem.* **2012**, *77* (24), 11167–11176.

(73) Szczepaniak, W.; Kuczynski, K. New Preparative Method for Aminomethylphosphonic, Aminoisopropylphosphonic and Iminobis(Methylenephosphonic) Acids. *Phosphorus and Sulfur and the Related Elements*. 1979, pp 333–337.

(74) *Méthodes d'analyse complexométriques avec les titriplex*; Merck E: Darmstadt, 1990.

(75) Raymond, K. Tragic Consequence with Acetonitrile Adduct. *Chem. Eng. News* **1983**, *61* (49), 4–4.

(76) Gans, P.; O'Sullivan, B. *GLEE*©; Protonic Softwares: Leeds, UK and Berkeley, CA, 2005.

(77) Gans, P.; O'Sullivan, B. GLEE, a New Computer Program for Glass Electrode Calibration. *Talanta* **2000**, *51* (1), 33–37.

(78) Gans, P.; Sabatini, A.; Vacca, A. Investigation of Equilibria in Solution. Determination of Equilibrium Constants with the HYPERQUAD Suite of Programs. *Talanta* **1996**, *43* (10), 1739–1753.

(79) Alderighi, L.; Gans, P.; Ienco, A.; Peters, D.; Sabatini, A.; Vacca, A. Hyperquad Simulation and Speciation (HySS): A Utility Program for the Investigation of Equilibria Involving Soluble and Partially Soluble Species. *Coord. Chem. Rev.* **1999**, *184*, 311–318.

(80) Gampp, H.; Maeder, M.; Meyer, C.; Zuberbuhler, A. Calculation of Equilibrium-Constants from Multiwavelength Spectroscopic Data .1. Mathematical Considerations. *Talanta* **1985**, *32* (2), 95–101.

(81) Cyrille Alliot; Michel, N.; Bonraisin, A.-C.; Bossé, V.; Laizé, J.; Bourdeau, C.; Mokili, B. M.; Haddad, F. One Step Purification Process for No-Carrier-Added ^{64}Cu Produced Using Enriched Nickel Target. *Radiochimica Acta*. 99th ed. 2011, pp 627–630.

(82) Bleiholder, C.; Börzel, H.; Comba, P.; Ferrari, R.; Heydt, M.; Kerscher, M.; Kuwata, S.; Laurenczy, G.; Lawrance, G. A.; Lienke, A.; Martin, B.; Merz, M.; Nuber, B.; Pritzkow, H. Coordination Chemistry of a New Rigid, Hexadentate Bispidine-Based Bis(Amine)Tetrakis(Pyridine) Ligand. *Inorg. Chem.* **2005**, *44* (22), 8145–8155.

(83) Comba, P.; Grimm, L.; Orvig, C.; Rück, K.; Wadepohl, H. Synthesis and Coordination Chemistry of Hexadentate Picolinic Acid Based Bispidine Ligands. *Inorg. Chem.* **2016**, *55* (24), 12531–12543.

(84) Meyer, M.; Frémond, L.; Tabard, A.; Espinosa, E.; Vollmer, G. Y.; Guilard, R.; Dory, Y. Synthesis, Characterization and X-Ray Crystal Structures of Cyclam Derivatives. Part VI. Proton Binding Studies of a Pyridine-Strapped 5,12-Dioxocyclam Based Macrobicycle. *New J. Chem.* **2005**, *29* (1), 99–108.

(85) Gans, P.; Sabatini, A.; Vacca, A. *HYPERQUAD2000*; Protonic Software, Leeds, U.K. and University of Florence, Italy, 2000.

(86) Siener, T.; Cambareri, A.; Kuhl, U.; Englberger, W.; Haurand, M.; Kögel, B.; Holzgrabe, U. Synthesis and Opioid Receptor Affinity of a Series of 2, 4-Diaryl-Substituted 3,7-Diazabicylononanones. *J. Med. Chem.* **2000**, *43* (20), 3746–3751.

(87) Kuhl, U.; Englberger, W.; Haurand, M.; Holzgrabe, U. Diazabicyclo[3.3.1]Nonanone-Type Ligands for the Opioid Receptors. *Arch. Pharm. Pharm. Med. Chem.* 2000, pp 226–230.

(88) Hosken, G. D.; Hancock, R. D. Very Strong and Selective Complexation of Small Metal Lons by a Highly Preorganised Open-Chain Bispidine-Based Ligand. *J. Chem. Soc. Chem. Commun.* **1994**, No. 11, 1363–1364.

(89) Lomozik, L. *Monatsh. Chem.* 1984, pp 261–270.

(90) Hathaway, B. J.; Billing, D. E. The Electronic Properties and Stereochemistry of Mono-Nuclear Complexes of the Copper(II) Ion. *Coord. Chem. Rev.* **1970**, *5* (2), 143–207.

(91) Patel, R. N.; Shrivastava, R. P.; Singh, N.; Kumar, S.; Pandeya, K. B. Equilibrium Studies on Mixed-Ligand Mixed-Metal Complexes of Copper(II), Nickel(II) and Zinc(II) with Glycylvaline and Imidazole. *Indian Journal of Chemistry.* 2001, pp 361–367.

(92) Clark, W. M. Oxidation-Reduction Potentials of Organic Systems. In *Encyclopedia of Electrochemistry of the Elements*; New York, 1976.

(93) Krebs, H. A.; Kornberg, H. L.; Burton, K. *Energy Transformations in Living Matter: A Survey*, Springer.; 1957.

(94) Lima, L. M. P.; Halime, Z.; Marion, R.; Camus, N.; Delgado, R.; Platas-Iglesias, C.; Tripier, R. Monopicolinate Cross-Bridged Cyclam Combining Very Fast Complexation with Very High Stability and Inertness of Its Copper(II) Complex. *Inorg. Chem.* **2014**, *53* (10), 5269–5279.

(95) Woodin, K. S.; Heroux, K. J.; Boswell, C. A.; Wong, E. H.; Weisman, G. R.; Niu, W.; Tomellini, S. A.; Anderson, C. J.; Zakharov, L. N.; Rheingold, A. L. Kinetic Inertness and Electrochemical Behavior of Copper(II) Tetraazamacrocyclic Complexes: Possible Implications for in Vivo Stability. *Eur. J. Inorg. Chem.* **2005**, *2005* (23), 4829–4833.

(96) Odendaal, A. Y.; Fiamengo, A. L.; Ferdani, R.; Wadas, T. J.; Hill, D. C.; Peng, Y.; Heroux, K. J.; Golen, J. A.; Rheingold, A. L.; Anderson, C. J.; Weisman, G. R.; Wong, E. H. Isomeric Trimethylene and Ethylene Pendant-Armed Cross-Bridged Tetraazamacrocycles and in Vitro/in Vivo Comparisions of Their Copper(II) Complexes. *Inorg. Chem.* **2011**, *50* (7), 3078–3086.

Synopsis – For Table of Content Only

A new hexadentate bispidol ligand with a pendant phosphonate group has been synthesized to be used for PET imaging. This ligand forms highly stable Cu(II) complexes with high kinetic inertness regarding reduction and acid-assisted dissociation. Quantitative radiolabelling was achieved within 5 min at room temperature at pH 4.6 and above and at submicromolar concentrations of ligand.

